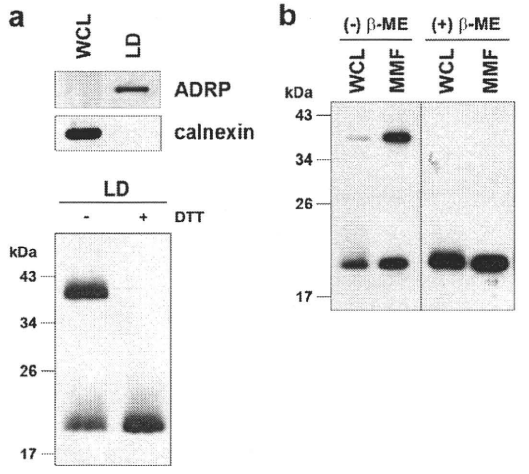

FIG. 3. The core complex is formed at the LD and ER. (a) The LD fraction and WCL were collected from JFH1^{E2FL} RNA-transfected HuH-7 cells on day 5 posttransfection. (upper panel) Immunoblot analysis of the LD marker ADRP and the ER marker calnexin in the LD fraction; (lower panel) immunoblot analysis of the core protein in the LD fraction treated or not treated with 50 mM DTT. (b) Immunoblot analysis of the core protein in the MMF and WCL collected from JFH1^{E2FL}-producing HuH-7 cells on day 5 posttransfection in the presence or absence of 5% β-ME. Data are representative of those from three independent experiments.

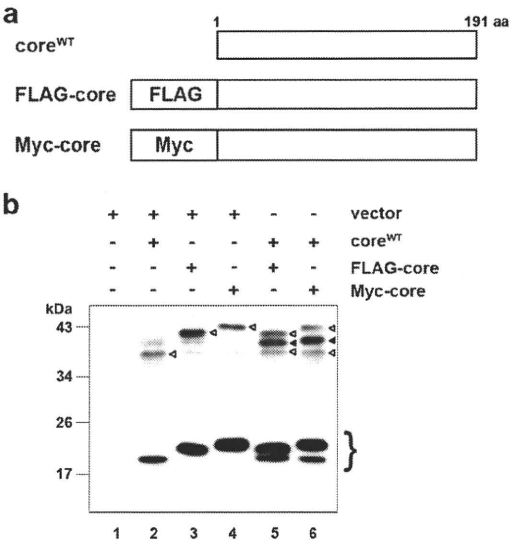

FIG. 4. The core complex consists of a core dimer. (a) Schematic of wild-type, FLAG-tagged (FLAG-core), and Myc-tagged (Myc-core) core proteins. (b) Immunoblot analysis of the core protein in the MMF collected from HuH-7 cells transfected with combinations of pcDNA3 (vector) and/or core expression plasmids (e.g., encoding core^{WT}, FLAG-core, and Myc-core), as indicated. The experiment was performed under nonreducing conditions. The lower bands represent core monomer (marked on the right with a brace). White arrowheads, bands corresponding to dbd-core; black arrowheads, positions of the intermediately sized core complex formed by core^{WT} and the tagged core. Data are representative of those from three independent experiments.

unknown reason (Fig. 1c, lanes 1 and 2). Although the intermolecular disulfide bond is known to be artificially formed in denaturing SDS-PAGE in the absence of reducing agents, the dbc-complex was still observed even in the presence of NEM, which is the alkylating agent for free sulfhydryls, during sample preparation (Fig. 2c), indicating that the dbc-complex was naturally present in the virus-like particles.

The HCV nucleocapsid is covered with lipid membranes and E1 and E2 proteins, making it resistant to proteases. As expected, in the absence of NP-40, the dbc-complex was resistant to proteinase K (Fig. 1c, lane 3), whereas proteinase K was able to digest core protein in whole-cell lysates (WCLs) collected from JFH1^{E2FL}-transfected HuH-7 cells (Fig. 1c, left panel). Disrupting the envelope structure with NP-40 made the dbc-complex susceptible to proteinase K treatment (Fig. 1c, lane 4), indicating that the dbc-complex was indeed a component of the HCV particle.

The dbc-complex forms on the ER. To investigate the subcellular site at which the dbc-complex forms, LDs and MMFs from JFH1^{E2FL} replicating HuH-7 cells were analyzed by immunoblotting. We first analyzed the dbc-complex in LDs, because LDs are involved in infectious HCV particle formation (36, 47). The purity of the LD fraction was determined using immunoblot analysis of calnexin and ADRP, ER and LD marker proteins, respectively (Fig. 3a, upper panel). The core protein was then analyzed in the LD fraction. As shown in Fig. 3a (lower panel), the dbc-complex was observed in the LD fraction from JFH1^{E2FL} RNA-transfected HuH-7 cells. We next analyzed the core protein in the ER-containing MMF, because the core protein is first translated and processed on the ER (16). As shown in Fig. 3b, the dbc-complex was observed in the MMF from JFH1^{E2FL} RNA-transfected HuH-7 cells. These results suggest that the dbc-complex is first formed at the ER. To assess the possibility that dbc-complex-containing HCV particles were also assembled on the ER, the sensitivity of the dbc-complex to protease treatment was analyzed. The dbc-complex in the MMF was susceptible to protease treatment in the absence of NP-40, indicating that the dbc-complex on the ER was not yet part of a HCV particle (data not shown).

dbc-complex is most likely a disulfide-bonded dimer form of the core. In order to examine whether the core protein itself has the potential to form a dbc-complex, we analyzed the dbc-complex formation of the full-length wild-type core protein (core^{WT}) expressed from pcDNA3-core^{WT} (36), the expression plasmid encoding the 191-amino-acid full-length core protein of JFH1 strain. We used this expression plasmid because the core protein from this plasmid was likely to be processed correctly enough to produce infectious HCV particles when it was cotransfected with the RNA of JFH1^{dc3}, which is a core protein deletion mutant of JFH1 (36). As a result, the dbc-complex formation was observed from the MMF of core^{WT}-expressing cells both in the absence and in the presence of NEM (Fig. 4b; lane 2 and data not shown, respectively). We next investigated the effect of the amino acid region of E1 on the production of the dbc-complex, because it has been reported that the efficient processing of core protein is dependent on the presence of some E1 sequence to ensure the insertion of the signal sequence for E1 in the translocon/membrane machinery (34). The dbc-complex was also observed

when the core protein was expressed from pcDNA3-C-E1/25, which encodes the full-length core protein followed by the N-terminal 25-amino-acid sequence of E1 to ensure that the core protein is processed properly (see Fig. S3a in the supplemental material). These data showed that the dbc-complex was formed by expression of the core protein only in the cells.

Next, we examined the structural components of the dbc-complex. Because the dbc-complex was twice the size of the core protein monomer, it was likely dbd-core. So, we investigated whether the core protein molecules with different tags were able to form the dbd-core. We first generated expression plasmids encoding core protein with the N-terminal FLAG and Myc tags (pcDNA3-FLAG-core and pcDNA3-Myc-core, respectively; Fig. 4a). The tagged core proteins were expressed or coexpressed with $core^{WT}$ in HuH-7 cells, and the MMF was analyzed by immunoblotting. The FLAG or Myc tag shifted the positions of the monomer and the complex bands (Fig. 4b, lanes 3 and 4) compared with the position of $core^{WT}$ (Fig. 4b, lane 2). When $core^{WT}$ was coexpressed with FLAG-core or Myc-core, the core protein complex of an intermediate size was observed, in addition to the bands obtained when the constructs were independently expressed (Fig. 4b, lanes 5 and 6, filled arrowheads); the intermediate-sized band disappeared after treatment with β-ME (see Fig. S3b, lanes 11 and 12, filled arrows, in the supplemental material), indicating that $core^{WT}$ and tagged core protein formed a heteromeric disulfide-bonded dimer. These results demonstrated that the dbc-complex on the ER is a dbd-core. Although we tried to detect the hetero- or homodimer consisting of the tagged core protein by using anti-FLAG or anti-Myc antibodies, these dimers were not detected, possibly because of the lower levels of sensitivity and specificity of the antibodies compared to those of the anti-core protein antibody that we used, especially against epitopes in the dbd-core. The results presented above, coupled with the similarities of the molecular sizes and sensitivities to β-ME and DTT, suggested that the dbc-complex in the HCV particle is most likely a dbd-core.

Core protein Cys128 mediates dbd-core formation. Our results showed that core protein from $JFH1^{E2FL}$ forms a disulfide-bonded dimer on the ER. A search for cysteine residues in the $JFH1^{E2FL}$ core protein identified amino acid positions 128 (Cys128) and 184 (Cys184) (see Fig. S1 in the supplemental material). These residues are highly conserved in core proteins from the approximately 2,000 reported HCV strains (HCVdb, http://www.hcvdb.org/, Hepatitis C Virus Database; http://s2as02.genes.nig.ac.jp/). To determine which cysteine residue mediated disulfide bond formation, we generated point mutations in $JFH1^{E2FL}$ that replaced Cys128 and/or Cys184 with alanine (Ala) (C128A, C184A, and C128/184A in $JFH1^{C128A}$, $JFH1^{C184A}$, and $JFH1^{C128/184A}$, respectively; Fig. 5a). As shown in Fig. 5b, the core proteins from $JFH1^{C128A}$ and $JFH1^{C128/184A}$ failed to form a dbd-core under nonreducing condition, whereas the core protein from $JFH1^{C184A}$ formed the dimer, indicating that Cys128 was the residue responsible. Similar results were observed when Cys was replaced by serine (Ser) instead of Ala (see Fig. S5c in the supplemental material). Recently, Majeau et al. reported that the core protein of the J6/JFH1 strain with Cys128 replacements by Ala or Ser were unstable in both *Pichia pastoris* and human hepatoma cell line HuH-7.5 (31), although we did not detect any noticeable degradation of the mutant core proteins of strain JFH1 (Fig. 5b; see also Fig. S5c in the supplemental material). This difference may have resulted from the difference in sample preparation methods, as we used the full-length genome of $JFH1^{E2FL}$ strain bearing the strain JFH1 core protein and HuH-7 cells instead of a core protein-expressing plasmid for the J6 strain and HuH-7.5 cells.

To exclude the possibility that mutation of Cys128 inhibited dbd-core formation by creating a conformational change, T127A and G129A core protein mutants ($JFH1^{T127A}$ and $JHF1^{G129A}$, respectively) were created and examined for their effects on dbd-core formation and infectious virus particle production. These mutants formed dbd-core, and infectious HCV particles were detected in the culture medium (see Fig. S4a to c in the supplemental material), supporting an essential role for Cys128 in dbd-core and particle formation.

dbd-core contributes to HCV particle production. To examine the functional roles of dbd-core, infectious HCV particle production, HCV replication efficiency, colocalization of the core protein and LDs, and RNA binding of mutant and wild-type ($JFH1^{E2FL}$) core protein were evaluated. Culture medium from HuH-7 cells transfected with $JFH1^{C128A}$ or $JFH1^{C128/184A}$ RNA contained significantly fewer infectious HCV particles compared with the numbers obtained with $JFH1^{E2FL}$ or $JFH1^{C184A}$ RNA (Fig. 5c). We also found significant decreases in the levels of HCV RNA and core protein in the culture medium of HuH-7 cells transfected with $JFH1^{C128A}$ or $JFH1^{C128/184A}$ RNA (Fig. 5d and e). Similar results were observed with J6/JFH1 C128A or the C128/184A mutant strain (data not shown). To investigate whether these results were due to suppressed HCV replication, the HCV RNA and protein levels in cells transfected with mutant RNA were analyzed using qRT-PCR and immunoblot analyses, respectively. Compared with the results obtained with $JFH1^{E2FL}$, no significant changes in the cellular HCV RNA titer at days 1, 3, and 5 posttransfection or in the expression of HCV nonstructural protein NS5A were observed (Fig. 6a and b). This indicated that substitution of Cys128 did not significantly affect HCV RNA genome replication or viral protein production, demonstrating that the dbd-core functions during HCV particle production rather than HCV genome replication. Similar results were observed using RNA of JFH1 mutant strain $JFH1^{C128S}$, in which the cysteine at position 128 was replaced by Ser instead of Ala (see Fig. S5a, b, and d in the supplemental material).

The subcellular localizations of the core protein and NS5A protein in HuH-7 cells transfected with HCV RNA were investigated using indirect immunofluorescence and confocal microscopy, because recruiting HCV proteins to LDs is an important step in infectious HCV particle production (36, 47) and core trafficking to LDs is dependent on signal peptide peptidase (SPP)-mediated cleavage of the tail region (34, 41). $JFH1^{C128A}$ mutant core protein and NS5A protein were efficiently trafficked to LDs, as was observed with wild-type $JHF1^{E2FL}$ (Fig. 6c), suggesting that SPP cleavage and core protein maturation were not affected by the C128A mutation. Similar results were obtained with the core proteins derived from $JFH1^{C184A}$ and $JFH1^{C128/184A}$ (see Fig. S6 in the supplemental material) and also Ser mutant $JFH1^{C128S}$ (see Fig. 5e in the supplemental material).

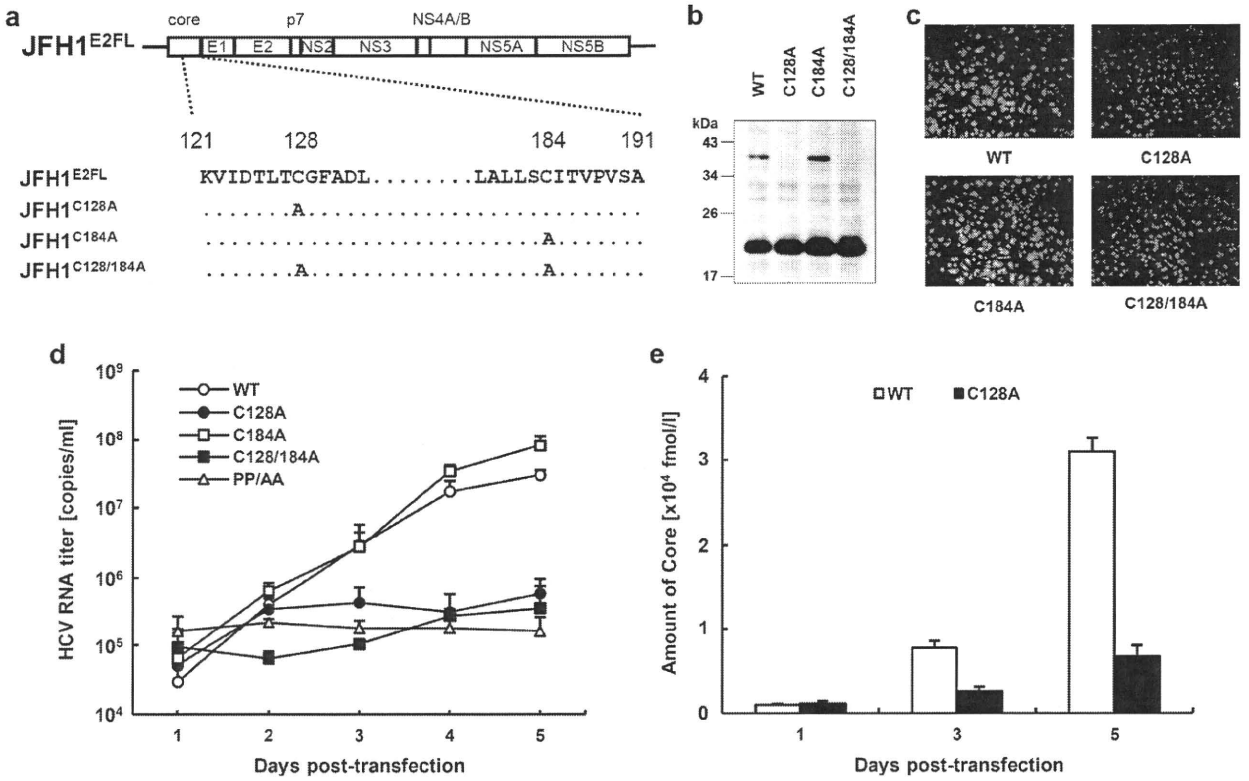

FIG. 5. The core dimer is formed via a bond between cysteine residues at amino acid position 128. (a) Site-directed mutagenesis of JFH1^{E2FL}. (b) Immunoblot analysis of the core protein in MMFs collected from HuH-7 cells under nonreducing conditions 3 days post-transfection with JFH1^{E2FL} (WT), JFH1^{C128A} (C128A), JFH1^{C184A} (C184A), or JFH1$^{C128/184A}$ (C128/184A) RNA. (c) Infectivity of culture medium collected and concentrated on day 5 posttransfection from HuH-7 cells transfected with WT, C128A, C184A, or C128/184A RNA. (d) Real-time qRT-PCR analysis of HCV RNA titers in culture medium collected at the indicated time points from HuH-7 cells transfected with WT, C128A, C184A, C128/184A, or PP/AA (JFH1$^{PP/AA}$) RNA. (e) ELISAs of core protein levels in culture medium collected at the indicated time points from HuH-7 cells transfected with WT or C128A RNA. Data are representative of those from three independent experiments (b and c) or are the means ± standard deviations from three independent experiments (d and e).

Because HCV core protein can bind to RNA, including the HCV genome, during viral particle assembly (43), we analyzed RNA binding by the core protein using *in vitro*-translated core^{C128A}, core^{WT}, and poly(U) agarose resin. Core^{C128A} and core^{WT} bound similarly to the poly(U) resin (Fig. 6d).

dbd-core is important for HCV particle assembly. The mutational analysis of the core protein indicated that core^{C128A} and core^{WT} similarly localize to LDs, recruit NS proteins to the LD, and bind to RNA. Moreover, this mutation did not markedly affect HCV genome replication. How does core^{C128A} affect the production of HCV particles? An important function of the core protein is multimerization, which is followed by capsid construction and packaging of the RNA genome in the viral particles. We therefore determined whether core^{C128A} had a dominant negative effect on virus-like particle production. Wild-type JFH1^{E2FL} RNA and different amounts of JFH1^{C128A} RNA were cotransfected into HuH-7 cells, and the HCV RNA titer and infectivity of the virus-like particles in the culture medium were analyzed. As expected, the HCV RNA titer in the cells increased with higher levels of transfected RNA (see Fig. S7a in the supplemental material). In contrast, the HCV RNA titer and infectivity in the culture medium decreased in a JFH1^{C128A} RNA dose-dependent manner when this mutant RNA was cotransfected with wild-type RNA (Fig. 7a, b). This suppressive effect was not observed when either wild-type RNA or core deletion mutant JFH1^{dc3} RNA was used instead of mutant RNA in a similar experiment (see Fig. S7b to e in the supplemental material), indicating that higher levels of HCV RNA alone did not inhibit HCV particle production. Thus, core^{C128A} had a dominant negative effect on HCV particle production. Together, these results suggest that dbd-core is involved in the assembly of HCV particles.

The nucleocapsid-like particle of HCV was resistant to trypsin treatment. To further investigate the structure of the HCV nucleocapsid-like particle most likely formed by dbd-core, we examined the sensitivity of the particle to trypsin, which cleaves polypeptides at the C-terminal end of basic residues. Whereas trypsin digested the core protein in the whole-cell lysates (Fig. 8a, left panel), dbd-core from buoyant density-fractionated JFH1^{E2FL} particles was resistant to digestion, despite NP-40 treatment (Fig. 8a, right panel), although it was sensitive to proteinase K, which has a broad specificity (Fig. 1c). The N-terminal hydrophilic domain of the core protein (from residues 6 to 121) contains a number of trypsin cleavage sites (25 sites

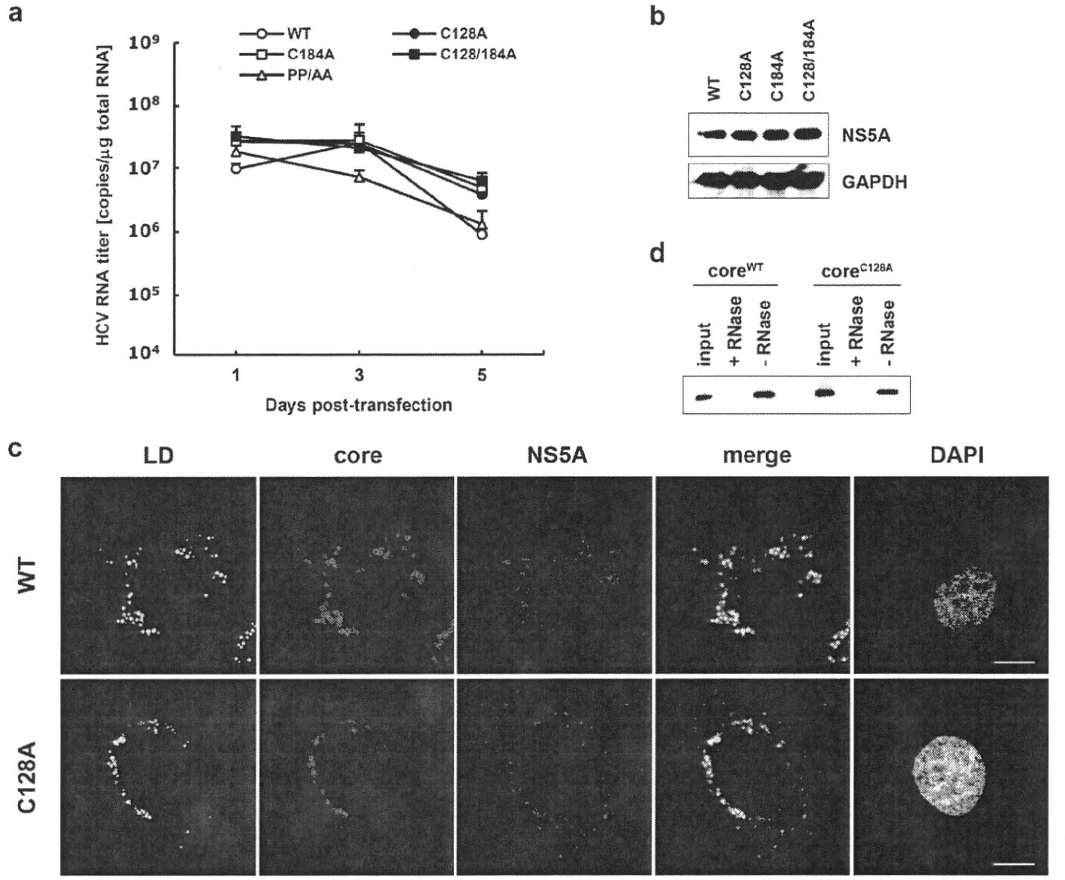

FIG. 6. Site-directed mutagenesis has no effect on HCV replication. (a) Real-time qRT-PCR analysis of the HCV RNA titer using total cellular RNA collected at the indicated time points from cells transfected with JFH1^{E2FL} (WT), JFH1^{C128A} (C128A), JFH1^{C184A} (C184A), JFH1$^{C128/184A}$ (C128/184A), or JFH1$^{PP/AA}$ (PP/AA) RNA. (b) Immunoblot analysis of NS5A protein and GAPDH in whole-cell lysate collected from cells transfected with WT, C128A, C184A, or C128/184A RNA at day 3 posttransfection. (c) Confocal microscopy of the subcellular localization of the LD (green), core (blue), NS5A protein (red), and nucleus (4′,6-diamidino-2-phenylindole [DAPI]) (gray) in WT and C128A replicating cells on day 3 posttransfection. Bars, 10 μm. (d) An RNA-protein binding precipitation assay was performed with *in vitro*-translated core^{WT} and core^{C128A} using poly(U) agarose as the resin. +RNase and −RNase, samples with and without RNase treatment, respectively, as described in Materials and Methods. Input indicates that 1/40 of the amount of translated product was used in this assay. Data represent the means ± standard deviations from three independent experiments (a) or are representative of those from three independent experiments (b to d).

in strain JHF1) (see Fig. S1 in the supplemental material), suggesting that the N-terminal domain faces inward and/or that the conformation prevents protease access. To address this idea, buoyant density-fractionated JFH1^{E2FL} particles were treated with trypsin under stricter conditions in the presence of NP-40. Cleavage of dbd-core by various levels of trypsin correlated with the appearance of a shorter molecule (Fig. 8b, white arrowhead). The shorter molecule was presumed to be partially digested dbd-core with an intact N-terminal region because it was recognized by anti-core protein antibodies, which bind to an epitope located from amino acids 20 to 40 of the core protein (M. Kohara, The Tokyo Metropolitan Institute of Medical Science, personal communication). These results suggest that dbd-core is assembled into the nucleocapsid-like particle such that most of the N-terminal domain is inside.

DISCUSSION

In the present study, we have shown that the nucleocapsid-like particle of HCV most likely contains a dimer of core protein that is stabilized by a disulfide bond. Mutational analysis revealed that Cys128 forms a disulfide bond between core monomers. Several reports have shown that disulfide bonds in the capsid proteins of some viruses are involved in virus particle assembly and stabilization of the viral capsid structure (4, 21, 27, 28, 57); these viruses are characterized by icosahedral nucleocapsids. Because, like these viruses, the HCV virion is spherical (2, 20), it has been suggested that HCV may contain a nucleocapsid with a similar structure (20). We found the dbc-complex, which is most likely to be the dbd-core in JFH1^{E2FL} virus-like particles (Fig. 1c and 8a). The dbd-core in the capsid structure was digested by proteinase K but not

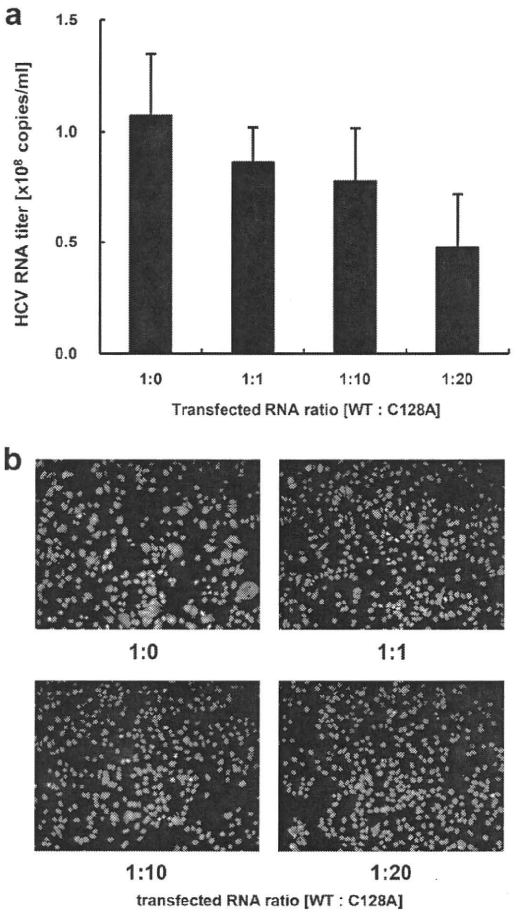

FIG. 7. JFH1^{C128A} core inhibits JFH1^{E2FL} particle assembly. A competitive inhibitory assay was performed with JFH1^{E2FL} (WT) and JFH1^{C128A} (C128A). (a) Real-time qRT-PCR analysis of the HCV RNA titer in HuH-7 cell culture medium 3 days after the cells were transfected with the indicated ratio of WT and C128A RNA. (b) The infectivity of culture medium collected from HuH-7 cells that had been transfected with the indicated ratio of WT and C128A RNA was analyzed as described in Materials and Methods. Data represent the means ± standard deviations from three independent experiments (a) or are representative of those from three independent experiments (b).

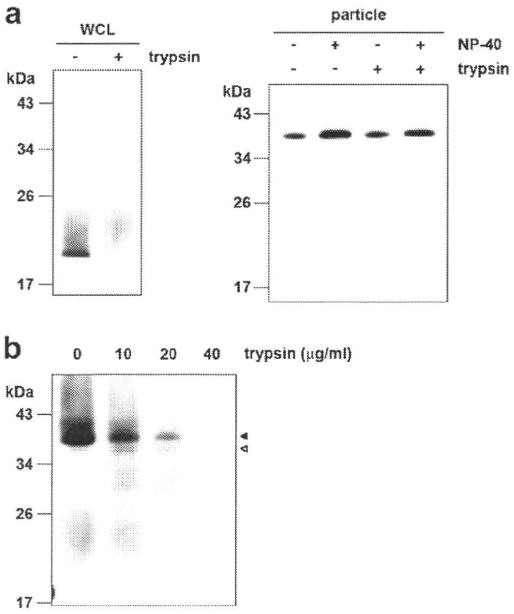

FIG. 8. The nucleocapsid-like particle of JFH1^{E2FL} is assembled with the C-terminal region of the core protein on the outer surface. (a) Immunoblot analysis of the core protein in JFH1^{E2FL} particles collected from sucrose density gradient fractions with high HCV RNA titers (particle) (Fig. 2a, fractions 8 to 13). The fractions were treated with 10 μg/ml trypsin at 37°C for 15 min in the presence or absence of 1% NP-40 (right panel). As a positive control, WCL prepared from JFH1^{E2FL} RNA-transfected HuH-7 cells in lysis buffer was treated with 10 μg/ml trypsin at 37°C for 15 min (left panel). (b) Immunoblot analysis of the core protein in JFH1^{E2FL} particles collected from sucrose density gradient fractions with high HCV RNA titers (Fig. 2a, fractions 8 to 13). The fractions were treated with the indicated concentrations of trypsin at 37°C for 10 min in the presence of 1% NP-40. Open and filled arrows indicate the positions of dbd-core and the trypsin-digested fragment, respectively. Data are representative of those from three independent experiments.

trypsin in the presence of NP-40 (Fig. 1c and 8a, lane 4). The resistance to trypsin suggested a tight conformation for dbd-core in the capsid and no exposed trypsin cleavage sites. The truncated form of dbd-core that was observed under certain trypsin treatment conditions likely resulted from cleavage in the C-terminal portion of the protein (e.g., arginine residues at positions 149 and 156) (see Fig. S1 in the supplemental material), although it is possible that the truncation of dbd-core was due to nonspecific cleavage by trypsin. These results imply that dbd-core is configured such that the N- and C-terminal ends are located at the inner and outer surfaces of the capsid, respectively. Because the N-terminal region of the core protein includes the RNA binding domain (43), the HCV RNA genome likely interacts with the core protein as it is packed in the nucleocapsid. On the other hand, the C-terminal hydrophobic domain probably faces the lipid membranes to form the envelope structure. Only part of the N-terminal hydrophilic region of the core protein has been structurally examined using X-ray crystal structural analysis (35) and structural bioinformatics and nuclear magnetic resonance analysis (11). Although the C-terminal half of the core protein has been structurally investigated by the use of bioinformatics (8), the three-dimensional structure containing the Cys128 residue is unknown. Thus, determination of the structure of the core protein in the nucleocapsid containing the Cys128 residue should be required for understanding the whole structure of this protein in the virus particles.

Because cotransfection of JFH1^{C128A} RNA with wild-type JFH1^{E2FL} RNA inhibited particle production in a mutant RNA dose-dependent manner (Fig. 7a and b), the C128A core variant clearly inhibited HCV particle formation by wild-type core protein. Cys128 was also previously reported to be a residue included in the region important for the production of infectious HCV (39). This residue is located near the N-terminal end of the hydrophobic region of the core (amino acids 122 to 177) and belongs to the hydrophilic side of an amphipathic helix expected to interact in the plane of the membrane interface (7). Therefore, it is possible to think that dbd-core

formation via Cys128 can stabilize the interaction between the core protein and the membranes. The N-terminal half of the core protein (amino acids 1 to 124) reportedly assembles into nucleocapsid-like particles in the presence of the 5′ UTR from HCV RNA (24), suggesting that some nucleocapsid-like particles may assemble via only homotypic interactions from the core protein. In addition to weak homotypic interactions, the HCV core protein forms a disulfide bond to stabilize the capsid structure, thus making dbd-core indispensable in the stable virus-like particle. We observed that culture medium from JFH1^{C128A}- or JFH1^{C128S}-transfected cells included slight infectivity (Fig. 5c; see also Fig. S5d in the supplemental material). This made us speculate that this mutant may produce some infective particle-like structure formed by a homotypic interaction of the core. Such a slight infectivity may have reflected the optimized *in vitro* culture conditions compared with the *in vivo* conditions, allowing relatively unstable virus particles to survive.

A nucleocapsid must be resistant to environmental degradation yet still be able to disassemble after infection. Disulfide bonds could help with this process by switching between a stable and unstable virus capsid on the basis of different intracellular and extracellular oxidation conditions (12, 30). During the virus life cycle, the disulfide bond strengthens the viral capsid structure and protects the viral genome from oxidative conditions and cellular nucleases when virus particles are formed. Upon infection, the disulfide bond may be cleaved under cytoplasmic reducing conditions, thereby releasing the viral genome into the cell for replication. HCV may utilize the core protein disulfide bond in this way as HCV enters the host cell via clathrin-mediated endocytosis (5) into a low-pH, endosomal compartment (25, 52); this is presumably followed by endosomal membrane fusion and release of the viral capsid into the cytoplasm (38).

Treatment of HCV infection with pegylated interferon in combination with ribavirin is not effective for all patients. Recently, drugs targeting viral proteins NS3/4A and NS5B have been examined in clinical trials. Although these drugs are relatively specific, resulting in fewer side effects and potent antiviral activity, monotherapy can be complicated by rapidly emerging resistant variants carrying mutations that reduce drug efficacy, perhaps due to conformational changes in the target (23, 48, 51). Therefore, viral proteins that are highly conserved among strains and those characterized by low mutation rates may be better targets for drug development. Because the core protein is the most conserved HCV protein and Cys128 is conserved among almost all HCV strains examined, drugs that interact with Cys128 and/or the region around or near this residue will likely show broad-spectrum efficacy to block stable infectious particle formation. Structural analysis of dbd-core should aid with the development of new STAT-Cs that target Cys128 by direct interaction with the sulfide group and/or region around this residue. Until now and still, the mechanism of disulfide bond formation of the core protein on the ER is unknown. Dimerization of the capsid protein by disulfide bond has been reported in some enveloped viruses (9, 19, 54, 56), although some were shown not to be important for virus particle formation (26, 55). Unlike vaccinia virus (46), no redox system of its own has been reported for these viruses. Therefore, further investigations addressing the mechanisms underlying dbd-core formation on the ER may reveal a new mechanism for disulfide bond formation of viral proteins in infected cells.

ACKNOWLEDGMENTS

This work was supported by grants-in-aid from the Ministry of Health, Labor, and Welfare of Japan and by grants-in-aid from the Japan Health Sciences Foundation.

REFERENCES

1. **Abid, K., V. Pazienza, A. de Gottardi, L. Rubbia-Brandt, B. Conne, P. Pugnale, C. Rossi, A. Mangia, and F. Negro.** 2005. An in vitro model of hepatitis C virus genotype 3a-associated triglycerides accumulation. J. Hepatol. **42**:744–751.
2. **Aly, H. H., Y. Qi, K. Atsuzawa, N. Usuda, Y. Takada, M. Mizokami, K. Shimotohno, and M. Hijikata.** 2009. Strain-dependent viral dynamics and virus-cell interactions in a novel in vitro system supporting the life cycle of blood-borne hepatitis C virus. Hepatology **50**:689–696.
3. **Asselah, T., Y. Benhamou, and P. Marcellin.** 2009. Protease and polymerase inhibitors for the treatment of hepatitis C. Liver Int. **29**(Suppl. 1):57–67.
4. **Baron, M. D., and K. Forsell.** 1991. Oligomerization of the structural proteins of rubella virus. Virology **185**:811–819.
5. **Blanchard, E., S. Belouzard, L. Goueslain, T. Wakita, J. Dubuisson, C. Wychowski, and Y. Rouille.** 2006. Hepatitis C virus entry depends on clathrin-mediated endocytosis. J. Virol. **80**:6964–6972.
6. **Boulant, S., M. W. Douglas, L. Moody, A. Budkowska, P. Targett-Adams, and J. McLauchlan.** 2008. Hepatitis C virus core protein induces lipid droplet redistribution in a microtubule- and dynein-dependent manner. Traffic **9**:1268–1282.
7. **Boulant, S., R. Montserret, R. G. Hope, M. Ratinier, P. Targett-Adams, J. P. Lavergne, F. Penin, and J. McLauchlan.** 2006. Structural determinants that target the hepatitis C virus core protein to lipid droplets. J. Biol. Chem. **281**:22236–22247.
8. **Boulant, S., C. Vanbelle, C. Ebel, F. Penin, and J. P. Lavergne.** 2005. Hepatitis C virus core protein is a dimeric alpha-helical protein exhibiting membrane protein features. J. Virol. **79**:11353–11365.
9. **Cornillez-Ty, C. T., and D. W. Lazinski.** 2003. Determination of the multimerization state of the hepatitis delta virus antigens in vivo. J. Virol. **77**:10314–10326.
10. **Dustin, L. B., and C. M. Rice.** 2007. Flying under the radar: the immunobiology of hepatitis C. Annu. Rev. Immunol. **25**:71–99.
11. **Duvignaud, J. B., C. Savard, R. Fromentin, N. Majeau, D. Leclerc, and S. M. Gagne.** 2009. Structure and dynamics of the N-terminal half of hepatitis C virus core protein: an intrinsically unstructured protein. Biochem. Biophys. Res. Commun. **378**:27–31.
12. **Freedman, R. B., B. E. Brockway, and N. Lambert.** 1984. Protein disulphide-isomerase and the formation of native disulphide bonds. Biochem. Soc. Trans. **12**:929–932.
13. **Giannini, C., and C. Brechot.** 2003. Hepatitis C virus biology. Cell Death Differ. **10**(Suppl. 1):S27–S38.
14. **Grakoui, A., C. Wychowski, C. Lin, S. M. Feinstone, and C. M. Rice.** 1993. Expression and identification of hepatitis C virus polyprotein cleavage products. J. Virol. **67**:1385–1395.
15. **Higashi, Y., H. Itabe, H. Fukase, M. Mori, Y. Fujimoto, R. Sato, T. Imanaka, and T. Takano.** 2002. Distribution of microsomal triglyceride transfer protein within sub-endoplasmic reticulum regions in human hepatoma cells. Biochim. Biophys. Acta **1581**:127–136.
16. **Hijikata, M., N. Kato, Y. Ootsuyama, M. Nakagawa, and K. Shimotohno.** 1991. Gene mapping of the putative structural region of the hepatitis C virus genome by in vitro processing analysis. Proc. Natl. Acad. Sci. U. S. A. **88**:5547–5551.
17. **Hijikata, M., H. Mizushima, Y. Tanji, Y. Komoda, Y. Hirowatari, T. Akagi, N. Kato, K. Kimura, and K. Shimotohno.** 1993. Proteolytic processing and membrane association of putative nonstructural proteins of hepatitis C virus. Proc. Natl. Acad. Sci. U. S. A. **90**:10773–10777.
18. **Hope, R. G., and J. McLauchlan.** 2000. Sequence motifs required for lipid droplet association and protein stability are unique to the hepatitis C virus core protein. J. Gen. Virol. **81**:1913–1925.
19. **Hu, H. M., K. N. Shih, and S. J. Lo.** 1996. Disulfide bond formation of the in vitro-translated large antigen of hepatitis D virus. J. Virol. Methods **60**:39–46.
20. **Ishida, S., M. Kaito, M. Kohara, K. Tsukiyama-Kohora, N. Fujita, J. Ikoma, Y. Adachi, and S. Watanabe.** 2001. Hepatitis C virus core particle detected by immunoelectron microscopy and optical rotation technique. Hepatol. Res. **20**:335–347.
21. **Jeng, K. S., C. P. Hu, and C. M. Chang.** 1991. Differential formation of disulfide linkages in the core antigen of extracellular and intracellular hepatitis B virus core particles. J. Virol. **65**:3924–3927.
22. **Kato, N., M. Hijikata, Y. Ootsuyama, M. Nakagawa, S. Ohkoshi, T. Sug-**

imura, and K. Shimotohno. 1990. Molecular cloning of the human hepatitis C virus genome from Japanese patients with non-A, non-B hepatitis. Proc. Natl. Acad. Sci. U. S. A. **87**:9524–9528.
23. **Kieffer, T. L., A. D. Kwong, and G. R. Picchio.** 2010. Viral resistance to specifically targeted antiviral therapies for hepatitis C (STAT-Cs). J. Antimicrob. Chemother. **65**:202–212.
24. **Kim, M., Y. Ha, and H. J. Park.** 2006. Structural requirements for assembly and homotypic interactions of the hepatitis C virus core protein. Virus Res. **122**:137–143.
25. **Koutsoudakis, G., A. Kaul, E. Steinmann, S. Kallis, V. Lohmann, T. Pietschmann, and R. Bartenschlager.** 2006. Characterization of the early steps of hepatitis C virus infection by using luciferase reporter viruses. J. Virol. **80**:5308–5320.
26. **Lee, J. Y., D. Hwang, and S. Gillam.** 1996. Dimerization of rubella virus capsid protein is not required for virus particle formation. Virology **216**:223–227.
27. **Li, M., P. Beard, P. A. Estes, M. K. Lyon, and R. L. Garcea.** 1998. Intercapsomeric disulfide bonds in papillomavirus assembly and disassembly. J. Virol. **72**:2160–2167.
28. **Li, P. P., A. Nakanishi, S. W. Clark, and H. Kasamatsu.** 2002. Formation of transitory intrachain and interchain disulfide bonds accompanies the folding and oligomerization of simian virus 40 Vp1 in the cytoplasm. Proc. Natl. Acad. Sci. U. S. A. **99**:1353–1358.
29. **Liang, T. J., L. J. Jeffers, K. R. Reddy, M. De Medina, I. T. Parker, H. Cheinquer, V. Idrovo, A. Rabassa, and E. R. Schiff.** 1993. Viral pathogenesis of hepatocellular carcinoma in the United States. Hepatology **18**:1326–1333.
30. **Liljas, L.** 1999. Virus assembly. Curr. Opin. Struct. Biol. **9**:129–134.
31. **Majeau, N., R. Fromentin, C. Savard, M. Duval, M. J. Tremblay, and D. Leclerc.** 2009. Palmitoylation of hepatitis C virus core protein is important for virion production. J. Biol. Chem. **284**:33915–33925.
32. **Matsumoto, M., S. B. Hwang, K. S. Jeng, N. Zhu, and M. M. Lai.** 1996. Homotypic interaction and multimerization of hepatitis C virus core protein. Virology **218**:43–51.
33. **McLauchlan, J.** 2000. Properties of the hepatitis C virus core protein: a structural protein that modulates cellular processes. J. Viral Hepat. **7**:2–14.
34. **McLauchlan, J., M. K. Lemberg, G. Hope, and B. Martoglio.** 2002. Intramembrane proteolysis promotes trafficking of hepatitis C virus core protein to lipid droplets. EMBO J. **21**:3980–3988.
35. **Menez, R., M. Bossus, B. H. Muller, G. Sibai, P. Dalbon, F. Ducancel, C. Jolivet-Reynaud, and E. A. Stura.** 2003. Crystal structure of a hydrophobic immunodominant antigenic site on hepatitis C virus core protein complexed to monoclonal antibody 19D9D6. J. Immunol. **170**:1917–1924.
36. **Miyanari, Y., K. Atsuzawa, N. Usuda, K. Watashi, T. Hishiki, M. Zayas, R. Bartenschlager, T. Wakita, M. Hijikata, and K. Shimotohno.** 2007. The lipid droplet is an important organelle for hepatitis C virus production. Nat. Cell Biol. **9**:1089–1097.
37. **Moradpour, D., C. Englert, T. Wakita, and J. R. Wands.** 1996. Characterization of cell lines allowing tightly regulated expression of hepatitis C virus core protein. Virology **222**:51–63.
38. **Moradpour, D., F. Penin, and C. M. Rice.** 2007. Replication of hepatitis C virus. Nat. Rev. Microbiol. **5**:453–463.
39. **Murray, C. L., C. T. Jones, J. Tassello, and C. M. Rice.** 2007. Alanine scanning of the hepatitis C virus core protein reveals numerous residues essential for production of infectious virus. J. Virol. **81**:10220–10231.
40. **Nolandt, O., V. Kern, H. Muller, E. Pfaff, L. Theilmann, R. Welker, and H. G. Krausslich.** 1997. Analysis of hepatitis C virus core protein interaction domains. J. Gen. Virol. **78**(Pt 6):1331–1340.
41. **Okamoto, K., Y. Mori, Y. Komoda, T. Okamoto, M. Okochi, M. Takeda, T. Suzuki, K. Moriishi, and Y. Matsuura.** 2008. Intramembrane processing by signal peptide peptidase regulates the membrane localization of hepatitis C virus core protein and viral propagation. J. Virol. **82**:8349–8361.
42. **Sabile, A., G. Perlemuter, F. Bono, K. Kohara, F. Demaugre, M. Kohara, Y. Matsuura, T. Miyamura, C. Brechot, and G. Barba.** 1999. Hepatitis C virus core protein binds to apolipoprotein AII and its secretion is modulated by fibrates. Hepatology **30**:1064–1076.
43. **Santolini, E., G. Migliaccio, and N. La Monica.** 1994. Biosynthesis and biochemical properties of the hepatitis C virus core protein. J. Virol. **68**:3631–3641.
44. **Seeff, L. B., and J. H. Hoofnagle.** 2003. Appendix: The National Institutes of Health Consensus Development Conference Management of Hepatitis C 2002. Clin. Liver Dis. **7**:261–287.
45. **Sekine-Osajima, Y., N. Sakamoto, K. Mishima, M. Nakagawa, Y. Itsui, M. Tasaka, Y. Nishimura-Sakurai, C. H. Chen, T. Kanai, K. Tsuchiya, T. Wakita, N. Enomoto, and M. Watanabe.** 2008. Development of plaque assays for hepatitis C virus-JFH1 strain and isolation of mutants with enhanced cytopathogenicity and replication capacity. Virology **371**:71–85.
46. **Senkevich, T. G., C. L. White, E. V. Koonin, and B. Moss.** 2000. A viral member of the ERV1/ALR protein family participates in a cytoplasmic pathway of disulfide bond formation. Proc. Natl. Acad. Sci. U. S. A. **97**:12068–12073.
47. **Shavinskaya, A., S. Boulant, F. Penin, J. McLauchlan, and R. Bartenschlager.** 2007. The lipid droplet binding domain of hepatitis C virus core protein is a major determinant for efficient virus assembly. J. Biol. Chem. **282**:37158–37169.
48. **Shimakami, T., R. E. Lanford, and S. M. Lemon.** 2009. Hepatitis C: recent successes and continuing challenges in the development of improved treatment modalities. Curr. Opin. Pharmacol. **9**:537–544.
49. **Tellinghuisen, T. L., M. J. Evans, T. von Hahn, S. You, and C. M. Rice.** 2007. Studying hepatitis C virus: making the best of a bad virus. J. Virol. **81**:8853–8867.
50. **Tellinghuisen, T. L., and C. M. Rice.** 2002. Interaction between hepatitis C virus proteins and host cell factors. Curr. Opin. Microbiol. **5**:419–427.
51. **Thompson, A. J., and J. G. McHutchison.** 2009. Antiviral resistance and specifically targeted therapy for HCV (STAT-C). J. Viral Hepat. **16**:377–387.
52. **Tscherne, D. M., C. T. Jones, M. J. Evans, B. D. Lindenbach, J. A. McKeating, and C. M. Rice.** 2006. Time- and temperature-dependent activation of hepatitis C virus for low-pH-triggered entry. J. Virol. **80**:1734–1741.
53. **Wakita, T., T. Pietschmann, T. Kato, T. Date, M. Miyamoto, Z. Zhao, K. Murthy, A. Habermann, H. G. Krausslich, M. Mizokami, R. Bartenschlager, and T. J. Liang.** 2005. Production of infectious hepatitis C virus in tissue culture from a cloned viral genome. Nat. Med. **11**:791–796.
54. **Wootton, S. K., and D. Yoo.** 2003. Homo-oligomerization of the porcine reproductive and respiratory syndrome virus nucleocapsid protein and the role of disulfide linkages. J. Virol. **77**:4546–4557.
55. **Zhou, S., and D. N. Standring.** 1992. Cys residues of the hepatitis B virus capsid protein are not essential for the assembly of viral core particles but can influence their stability. J. Virol. **66**:5393–5398.
56. **Zhou, S., and D. N. Standring.** 1992. Hepatitis B virus capsid particles are assembled from core-protein dimer precursors. Proc. Natl. Acad. Sci. U. S. A. **89**:10046–10050.
57. **Zweig, M., C. J. Heilman, Jr., and B. Hampar.** 1979. Identification of disulfide-linked protein complexes in the nucleocapsids of herpes simplex virus type 2. Virology **94**:442–450.

JOURNAL OF VIROLOGY, June 2010, p. 5824–5835 Vol. 84, No. 11
0022-538X/10/$12.00 doi:10.1128/JVI.02397-09

Production of Infectious Hepatitis C Virus by Using RNA Polymerase I-Mediated Transcription▽

Takahiro Masaki,[1]† Ryosuke Suzuki,[1]† Mohsan Saeed,[1,4] Ken-ichi Mori,[2] Mami Matsuda,[1] Hideki Aizaki,[1] Koji Ishii,[1] Noboru Maki,[2] Tatsuo Miyamura,[1] Yoshiharu Matsuura,[3] Takaji Wakita,[1] and Tetsuro Suzuki[1]*

Department of Virology II, National Institute of Infectious Diseases, Shinjuku-ku, Tokyo 162-8640, Japan[1]; Advanced Life Science Institute, Wako, Saitama 351-0112, Japan[2]; Department of Molecular Virology, Research Institute for Microbial Diseases, Osaka University, Suita-shi, Osaka 565-0871, Japan[3]; and Graduate School of Medicine, The University of Tokyo, Tokyo 113-0033, Japan[4]

Received 13 November 2009/Accepted 8 March 2010

In this study, we used an RNA polymerase I (Pol I) transcription system for development of a reverse genetics protocol to produce hepatitis C virus (HCV), which is an uncapped positive-strand RNA virus. Transfection with a plasmid harboring HCV JFH-1 full-length cDNA flanked by a Pol I promoter and Pol I terminator yielded an unspliced RNA with no additional sequences at either end, resulting in efficient RNA replication within the cytoplasm and subsequent production of infectious virions. Using this technology, we developed a simple replicon *trans*-packaging system, in which transient transfection of two plasmids enables examination of viral genome replication and virion assembly as two separate steps. In addition, we established a stable cell line that constitutively produces HCV with a low mutation frequency of the viral genome. The effects of inhibitors of N-linked glycosylation on HCV production were evaluated using this cell line, and the results suggest that certain step(s), such as virion assembly, intracellular trafficking, and secretion, are potentially up- and downregulated according to modifications of HCV envelope protein glycans. This Pol I-based HCV expression system will be beneficial for a high-throughput antiviral screening and vaccine discovery programs.

Over 170 million people worldwide have been infected with hepatitis C virus (HCV) (22, 33, 37), and persistence of HCV infection is one of the leading causes of liver diseases, such as chronic hepatitis, cirrhosis, and hepatocellular carcinoma (16, 25, 38). The HCV genome is an uncapped 9.6-kb positive-strand RNA sequence consisting of a 5′ untranslated region (UTR), an open reading frame encoding at least 10 viral proteins (Core, E1, E2, p7, NS2, NS3, NS4A, NS4B, NS5A, and NS5B), and a 3′UTR (46). The structural proteins (Core, E1, and E2) reside in the N-terminal region.

The best available treatment for HCV infection, which is pegylated alpha interferon (IFN-α) combined with ribavirin, is effective in only about half of patients and is often difficult to tolerate (25). To date, a prophylactic or therapeutic vaccine is not available. There is an urgent need to develop more effective and better tolerated therapies for HCV infection. Recently, a robust system for HCV production and infection in cultured cells has been developed. The discovery that some HCV isolates can replicate in cell cultures and release infectious particles has allowed the complete viral life cycle to be studied (23, 49, 53). The most robust system for HCV production involves transfection of Huh-7 cells with genomic HCV RNA of the JFH-1 strain by electroporation. However, using this RNA transfection system, the amount of secreted infectious viruses often fluctuate and mutations emerge in HCV genome with multiple passages for an extended period of time (54), which limits its usefulness for antiviral screening and vaccine development.

DNA-based expression systems for HCV replication and virion production have also been examined (5, 15, 21). With DNA-based expression systems, transcriptional expression of functional full-length HCV RNA is controlled by an RNA polymerase II (Pol II) promoter and a self-cleaving ribozyme(s). DNA expression systems using RNA polymerase I (Pol I) have been utilized in reverse genetics approaches to replicate negative-strand RNA viruses, including influenza virus (12, 29), Uukuniemi virus (11), Crimean-Congo hemorrhagic fever virus (10), and Ebola virus (13). Pol I is a cellular enzyme that is abundantly expressed in growing cells and transcribes rRNA lacking both a 5′ cap and a 3′ poly(A) tail. Thus, viral RNA synthesized in cells transfected with Pol I-driven plasmids containing viral genomic cDNA has no additional sequences at the 5′- or 3′ end even in the absence of a ribozyme sequence (28). The advantages of DNA-based expression systems are that DNA expression plasmids are easier to manipulate and generate stable cell lines that constitutively express the viral genome.

We developed here a new HCV expression system based on transfection of an expression plasmid containing a JFH-1 cDNA clone flanked by Pol I promoter and terminator sequences to generate infectious HCV particles from transfected cells. The technology presented here has strong potential to be the basis for *trans*-encapsidation system by transient transfection of two plasmids and for the establishment of an efficient and reliable screening system for potential antivirals.

MATERIALS AND METHODS

DNA construction. To generate HCV-expressing plasmids containing full-length JFH1 cDNA embedded between Pol I promoter and terminator se-

* Corresponding author. Present address: Department of Infectious Diseases, Hamamatsu University School of Medicine, Hamamatsu 431-3192, Japan. Phone: 81-53-435-2336. Fax: 81-53-435-2337. E-mail: tesuzuki@hama-med.ac.jp.

† T.M. and R.S. contributed equally to this study.

▽ Published ahead of print on 17 March 2010.

quences, part of the 5′UTR region and part of the NS5B to the 3′UTR region of full-length JFH-1 cDNA were amplified by PCR using primers containing BsmBI sites. Each amplification product was then cloned into a pGEM-T Easy vector (Promega, Madison, WI) and verified by DNA sequencing. Both fragments were excised by digestion with NotI and BsmBI, after which they were cloned into the BsmBI site of the pIII121 vector (a gift from Yoshihiro Kawaoka, School of Veterinary Medicine, University of Wisconsin-Madison [29]), which contains a human Pol I promoter and a mouse Pol I terminator. The resultant plasmid was digested by AgeI and EcoRV and ligated to JFH-1 cDNA digested by AgeI and EcoRV to produce pHIIJFH1. pHIIJFH1/GND having a point mutation at the GDD motif in NS5B to abolish RNA-dependent RNA polymerase activity and pHIIJFH1/R783A/R785A carrying double Arg-to-Ala substitutions in the cytoplasmic loop of p7 were constructed by oligonucleotide-directed mutagenesis. To generate pHIIJFH1/ΔE carrying in-frame deletions of parts of the E1 and E2 regions (amino acids [aa] 256 to 567), pHIIJFH1 was digested with NcoI and AscI, followed by Klenow enzyme treatment and self-ligation. To generate pIII/SGR-Luc carrying the bicistronic subgenomic HCV reporter replicon and its replication-defective mutant, pHH/SGR-Luc/GND, AgeI-SpeI fragments of pHHJFH1 and pHIIJFH1/GND were replaced with an AgeI-SpeI fragment of pSGR-JFH1/Luc (20). In order to construct pCAG/C-NS2 and pCAG/C-p7, PCR-amplified cDNA for C-NS2 and C-p7 regions of the JFH-1 strain were inserted into the EcoRI sites of pCAGGS (30). In order to construct stable cell lines, a DNA fragment containing a Zeocin resistance gene excised from pSV2/Zeo2 (Invitrogen, Carlsbad, CA) was inserted into pIII21 (pIIIZeo). Full-length JFH-1 cDNA was then inserted into the BsmBI sites of pIIIZeo. The resultant construct was designated pHIIJFH1/Zeo.

Cells and compounds. The human hepatoma cell line, Huh-7, and its derivative cell line, Huh7.5.1 (a gift from Francis V. Chisari, The Scripps Research Institute), were maintained in Dulbecco modified Eagle medium (DMEM) supplemented with nonessential amino acids, 100 U of penicillin/ml, 100 μg of streptomycin/ml, and 10% fetal bovine serum (FBS) at 37°C in a 5% CO_2 incubator. *N*-Nonyl-deoxynojirimycin (*N*N-DNJ) and kifunensine (KIF) were purchased from Toronto Research Chemicals (Ontario, Canada), castanospermine (CST) and 1,4-dideoxy-1,4-imino-D-mannitol hydrochloride (DIM) were from Sigma-Aldrich (St. Louis, MO), 1-deoxymannojirimycin (DMJ) and swainsonine (SWN) were from Alexis Corp. (Lausen, Switzerland), and *N*-butyl-deoxynojirimycin (*N*B-DNJ) was purchased from Wako Chemicals (Osaka, Japan). BILN 2061 was a gift from Boehringer Ingelheim (Canada), Ltd. These compounds were dissolved in dimethyl sulfoxide and used for the experiments. IFN-α was purchased from Dainippon-Sumitomo (Osaka, Japan).

DNA transfection and selection of stable cell lines. DNA transfection was performed by using FuGENE 6 transfection reagent (Roche, Mannheim, German) in accordance with the manufacturer's instructions. To establish stable cell lines constitutively producing HCV particles, pHHJFH1/Zeo was transfected into Huh7.5.1 cells within 35-mm dishes. At 24 h posttransfection (p.t.), the cells were then divided into 100-mm dishes at various cell densities and incubated with DMEM containing 0.4 mg of zeocin/ml for approximately 3 weeks. Selected cell colonies were picked up and amplified. The expression of HCV proteins was confirmed by measuring secreted core proteins. The stable cell line established was designated H751JFH1/Zeo.

***In vitro* synthesis of HCV RNA and RNA transfection.** RNA synthesis and transfection were performed as previously described (26, 49).

RNA preparation, Northern blotting, and RNase protection assay (RPA). Total cellular RNA was extracted with a TRIzol reagent (Invitrogen), and HCV RNA was isolated from filtered culture supernatant by using the QIAamp viral RNA minikit (Qiagen, Valencia, CA). Extracted cellular RNA was treated with DNase (TURBO DNase; Ambion, Austin, TX) and cleaned up by using an RNeasy minikit, which includes another step of RNase-free DNase digestion (Qiagen). The cellular RNA (4 μg) was separated on 1% agarose gels containing formaldehyde and transferred to a positively charged nylon membrane (GE Healthcare, Piscataway, NJ). After drying and cross-linking by UV irradiation, hybridization was performed with [α-^{32}P]dCTP-labeled DNA using Rapid-Hyb buffer (GE Healthcare). The DNA probe was synthesized from full-length JFH-1 cDNA using the Megaprime DNA labeling system (GE Healthcare). Quantification of positive- and negative-strand HCV RNA was performed using the RPA with biotin-16-uridine-5′-triphosphate (UTP)-labeled HCV-specific RNA probes, which contain 265 nucleotides (nt) complementary to the positive-strand (+) 5′UTR and 248 nt complementary to the negative-strand (−) 3′UTR. Human β-actin RNA probes labeled with biotin-16-UTP were used as a control to normalize the amount of total RNA in each sample. The RPA was carried out using an RPA III kit (Ambion) according to the manufacturer's procedures. Briefly, 15 μg of total cellular RNA was used for hybridization with 0.3 ng of the β-actin probe and 0.6 ng of either the HCV (+) 5′UTR or (−) 3′UTR RNA probe. After digestion with RNase A/T1, the RNA products were analyzed by electrophoresis in a 6% polyacrylamide–8 M urea gel and visualized by using a chemiluminescent nucleic acid detection module (Thermo Scientific, Rockford, IL) according to the manufacturer's instructions.

Reverse transcriptase PCR (RT-PCR), sequencing, and rapid amplification of cDNA ends (RACE). Aliquots (5 μl) of RNA solution extracted from filtered culture supernatant were subjected to reverse transcription with random hexamer and Superscript II reverse transcriptase (Invitrogen). Four fragments of HCV cDNA (nt 129 to 2367, nt 2285 to 4665, nt 4574 to 7002, and nt 6949 to 9634), which covers most of the HCV genome, were amplified by nested PCR. Portions (1 or 2 μl) of each cDNA sample were subjected to PCR with TaKaRa LA *Taq* polymerase (Takara, Shiga, Japan). The PCR conditions consisted of an initial denaturation at 95°C for 2 min, followed by 30 cycles of denaturation at 95°C for 30 s, annealing at 60°C for 30 s, and extension at 72°C for 3 min. The amplified products were separated by agarose gel electrophoresis and used for direct DNA sequencing. To establish the 5′ ends of the HCV transcripts from pHHJFH1, a synthetic 45-nt RNA adapter (Table 1) was ligated to RNA extracted from the transfected cells 1 day p.t. using T4 RNA ligase (Takara). The viral RNA sequences were then reverse transcribed using SuperScript III reverse transcriptase (Invitrogen) with a primer, RT (Table 1). The resultant cDNA sequences were subsequently amplified by PCR with 5′RACEouter-S and 5′RACEouter-R primers, followed by a second cycle of PCR using 5′RACEinner-S and 5′RACEinner-R primers (Table 1). To establish the terminal 3′-end sequences, extracted RNA sequences were polyadenylated using a poly(A) polymerase (Takara), reverse transcribed with CAC-T35 primer (Table 1), and amplified with the primers 3X-10S (Table 1) and CAC-T35. The amplified 5′ and 3′ cDNA sequences were then separated by agarose gel electrophoresis, cloned into the pGEM-T Easy vector (Promega), and sequenced.

Western blotting. The proteins were transferred onto a polyvinylidene difluoride membrane (Immobilon; Millipore, Bedford, MA) after separation by SDS-PAGE. After blocking, the membranes were probed with a mouse monoclonal anti-HCV core antibody (2H9) (49), a rabbit polyclonal anti-NS5B antibody, or a mouse monoclonal GAPDH (glyceraldehyde-3-phosphate dehydrogenase) antibody (Chemicon, Temecula, CA), followed by incubation with a peroxidase-conjugated secondary antibody and visualization with an ECL Plus Western blotting detection system (Amersham, Buckinghamshire, United Kingdom).

Quantification of HCV core protein. HCV core protein was quantified by using a highly sensitive enzyme immunoassay (Ortho HCV antigen ELISA kit; Ortho Clinical Diagnostics, Tokyo, Japan) in accordance with the manufacturer's instructions.

Sucrose density gradient analysis. Samples of cell culture supernatant were processed by low-speed centrifugation and passage through a 0.45-μm-pore-size filter. The filtrated supernatant was then concentrated ~30-fold by ultrafiltration by using an Amicon Ultra-15 filter device with a cutoff molecular mass of 100,000 kDa (Millipore), after which it was layered on top of a continuous 10 to 60% (wt/vol) sucrose gradient, followed by centrifugation at 35,000 rpm at 4°C for 14 h with an SW41 rotor (Beckman Coulter, Fullerton, CA). Fractions of 1 ml were collected from the bottom of the gradient. The core level and infectivity of HCV in each fraction were determined.

Quantification of HCV infectivity. Infectious virus titration was performed by a 50% tissue culture infectious dose ($TCID_{50}$) assay, as previously described (23, 26). Briefly, naive Huh7.5.1 cells were seeded at a density of 10^4 cells/well in a 96-well flat-bottom plate 24 h prior to infection. Five serial dilutions were performed, and the samples were used to infect the seeded cells (six wells per dilution). At 72 h after infection, the inoculated cells were fixed and immunostained with a rabbit polyclonal anti-NS5A antibody (14), followed by an Alexa Fluor 488-conjugated anti-rabbit secondary antibody (Invitrogen).

Labeling of *de novo*-synthesized viral RNA and immunofluorescence staining. Labeling of *de novo*-synthesized viral RNA was performed as previously described with some modifications (40). Briefly, cells were plated onto an eight-well chamber slide at a density of 5×10^4 cells/well. One day later, the cells were incubated with actinomycin D at a final concentration of 10 μg/ml for 1 h and washed twice with HEPES-saline buffer. Bromouridine triphosphate (BrUTP) at 2 mM was subsequently transfected into the cells using FuGENE 6 transfection reagent, after which the cells were incubated for 15 min on ice. After the cells were washed twice with phosphate-buffered saline (PBS), they were incubated in fresh DMEM supplemented with 10% FBS at 37°C for 4 h. The cells were then fixed with 4% paraformaldehyde for 20 min and permeabilized with PBS containing 0.1% Triton X-100 for 15 min at room temperature. Immunofluorescence staining of NS5A and *de novo*-synthesized HCV RNA was performed as previously described (26, 40). The nuclei were stained with DAPI (4′,6′-diamidino-2-phenylindole) solution (Sigma-Aldrich). Confocal microscopy was performed

TABLE 1. Oligonucleotides used for RT-PCR and RACE of the JFH-1 genome

Method or segment	Oligonucleotide	Sequences (5′–3′)
5′RACE	RT	GTACCCCATGAGGTCGGCAAAG
	45-nt RNA adapter	GCUGAUGGCGAUGAAUGAACACUGCGUUUGCUGGCUUUGAUGAAA
	5′RACEouter-S	GCTGATGGCGATGAATGAACACTG
	5′RACEouter-R	GACCGCTCCGAAGTTTTCCTTG
	5′RACEinner-S	GAACACTGCGTTTGCTGGCTTTGATG
	5′RACEinner-R	CGCCCTATCAGGCAGTACCACAAG
3′RACE	CAC-T35	CACTTTTTTTTTTTTTTTTTTTTTTTTTTTTTTTT
	3X-10S	ATCTTAGCCCTAGTCACGGC
nt 129-2367	44S (1st PCR)	CTGTGAGGAACTACTGTCTT
	2445R	TCCACGATGTTCTGGTGAAG
	17S (2nd PCR)	CGGGAGAGCCATAGTGG
	2367R	CATTCCGTGGTAGAGTGCA
nt 2285-4665	2099S (1st PCR)	ACGGACTGTTTTAGGAAGCA
	4706R	TTGCAGTCGATCACGGAGTC
	2285S (2nd PCR)	AACTTCACTCGTGGGGATCG
	4665R	TCGGTGGCGACGACCAC
nt 4574-7002	4547S (1st PCR)	AAGTGTGACGAGCTCGCGG
	7027R	CATGAACAGGTTGGCATCCACCAT
	4594S (2nd PCR)	CGGGGTATGGGCTTGAACGC
	7003R	GTGGTGCAGGTGGCTCGCA
nt 6949-9634	6881S (1st PCR)	ATTGATGTCCATGCTAACAG
	3X-75R	TACGGCACTCTCTGCAGTCA
	6950S (2nd PCR)	GAGCTCCTCAGTGAGCCAG
	3X-54R	GCGGCTCACGGACCTTTCAC

using a Zeiss confocal laser scanning microscope LSM 510 (Carl Zeiss, Oberkochen, Germany).

Luciferase assay. Huh7.5.1 cells were seeded onto a 24-well cell culture plate at a density of 3×10^4 cells/well 24 h prior to inoculation with 100 μl of supernatant from the transfected cells. The cells were incubated for 72 h, followed by lysis with 100 μl of lysis buffer. The luciferase activity of the cells was determined by using a luciferase assay system (Promega). All luciferase assays were done at least in triplicate. For the neutralization experiments, a mouse monoclonal anti-CD81 antibody (JS-81; BD Pharmingen, Franklin Lakes, NJ) and a mouse monoclonal anti-FLAG antibody (Sigma-Aldrich) were used.

Flow cytometric analysis. Cells detached by treatment with trypsin were incubated in PBS containing 1% (vol/vol) formaldehyde for 15 min. A total of 5×10^5 cells were resuspended in PBS and treated with or without 0.75 μg of anti-CD81 antibody for 30 min at 4°C. After being washed with PBS, the cells were incubated with an Alexa Fluor 488-conjugated anti-mouse secondary antibody (Invitrogen) at 1:200 for 30 min at 4°C, washed repeatedly, and resuspended in PBS. Analyses were performed by using FACSCalibur system (Becton Dickinson, Franklin Lakes, NJ).

RESULTS

Analysis of the 5′ and 3′ ends of HCV RNA sequences generated from Pol I-driven plasmids. To examine whether the HCV transcripts generated from Pol I-driven plasmids had correct nucleotides at the 5′ and 3′ ends, we extracted RNA from Huh-7 cells transfected with pHHJFH1, which carries a genome-length HCV cDNA with a Pol I promoter/terminator, as well as from the culture supernatants. After this, the nucleotide sequences at both ends were determined using RACE and sequence analysis. A 328-nt fragment corresponding to cDNA from the 5′ end of HCV RNA was detected in the cell samples (Fig. 1A). Cloning of amplified fragments confirmed that the HCV transcripts were initiated from the first position of the viral genome in all of the clones sequenced (Fig. 1B). Similarly, a 127-nt amplification fragment was detected in each sample by 3′RACE (Fig. 1C), and the same 3′-end nucleotide sequence was observed in all clones derived from the culture supernatant (Fig. 1D, left). An additional two nucleotides (CC) were found at the 3′ end of the HCV transcript in a limited number of sequences (1 of 11 clones) derived from the cell sample (Fig. 1D, right), which were possibly derived from the Pol I terminator sequence by incorrect termination. These results indicate that most HCV transcripts generated from the Pol I-based HCV cDNA expression system are faithfully processed, although it is not determined whether the 5′ terminus of the viral RNA generated from Pol I system is triphosphate or monophosphate. It can be speculated that viral RNA lacking modifications at the 5′ and 3′ ends is preferentially packaged and secreted into the culture supernatant.

Production of HCV RNA, proteins, and virions from cells transiently transfected with Pol I-driven plasmids. To examine HCV RNA replication and protein expression in cells transfected with pHHJFH1, pHHJFH1/GND, or virion production-defective mutants, pHHJFH1/ΔE and pHHJFH1/R783A/R785A, which possess an in-frame deletion of E1/E2 region and substitutions in the p7 region, respectively (19, 42, 49), RPA and Western blotting were performed 5 days p.t. (Fig. 2A, B, and D). Positive-strand HCV RNA sequences were more abundant than negative-strand RNA sequences in these cells. Positive-strand RNA, but not negative-strand RNA, was detected in cells transfected with the replication-defective mutant pHHJFH1/GND (Fig. 2A and B). Northern blotting showed that genome-length RNA was generated in pHHJFH1-transfected cells but not in pHHJFH1/GND-transfected cells (Fig. 2C).

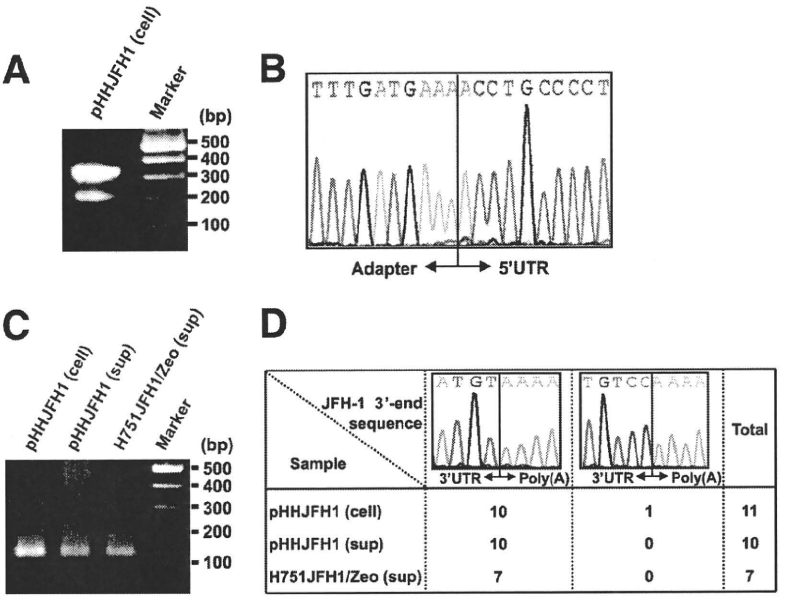

FIG. 1. Determination of the nucleotide sequences at the 5′-and 3′ ends of HCV RNA produced by the Pol I system. (A and B) 5′RACE and sequence analysis. A synthesized RNA adapter was ligated to RNA extracted from cells transfected with pHHJFH1. The positive-strand HCV RNA was reverse transcribed, and the resulting cDNA was amplified by nested PCR. The amplified 5′-end cDNA was separated by agarose gel electrophoresis (A), cloned, and sequenced (B). (C and D) 3′RACE and sequence analysis. RNA extracted from pHHJFH1-transfected cells, the culture supernatant of transfected cells, and the culture supernatant of H751JFH1/Zeo cells were polyadenylated, reverse transcribed, and amplified by PCR. The amplified 3′-end cDNA was separated by agarose gel electrophoresis (C), cloned, and sequenced (D).

As shown in Fig. 2D, the intracellular expression of core and NS5B proteins was comparable among cells transfected with pHHJFH1, pHHJFH1/ΔE, and pHHJFH1/R783A/R785A. Neither viral protein was detected in pHHJFH1/GND-transfected cells, suggesting that the level of viral RNA generated transiently from the DNA plasmid does not produce enough HCV proteins for detection and that ongoing amplification of the HCV RNA by the HCV NS5B polymerase allows a high enough level of viral RNA to produce detectable levels of HCV proteins.

To assess the release of HCV particles from cells transfected with Pol I-driven plasmids, core protein was quantified in culture supernatant by enzyme-linked immunosorbent assay (ELISA) or sucrose density gradient centrifugation. Core protein secreted from pHHJFH1-transfected cells was first detectable 2 days p.t., with levels increasing up to ~4 pmol/liter on day 6 (Fig. 3A). This core protein level was 4- to 6-fold higher than that in the culture supernatant of pHHJFH1/ΔE- or pHHJFH1/R783A/R785A-transfected cells, despite comparable intracellular core protein levels (Fig. 2D). Core protein was not secreted from cells transfected with pHHJFH1/GND (Fig. 3A). In another experiment, a plasmid expressing the secreted form of human placental alkaline phosphatase (SEAP) was cotransfected with each Pol I-driven plasmid. SEAP activity in culture supernatant was similar among all transfection groups, indicating comparable efficiencies of transfection (data not shown). Sucrose density gradient analysis of the concentrated supernatant of pHHJFH1-transfected cells indicated that the distribution of core protein levels peaked in the fraction of 1.17 g/ml density, while the peak of infectious titer was observed in the fraction of 1.12 g/ml density (Fig. 3B), which is consistent with the results of previous studies based on JFH-1-RNA transfection (23).

We next compared the kinetics of HCV particle secretion in the Pol I-driven system and RNA transfection system. Huh-7 cells, which have limited permissiveness for HCV infection (2), were transfected with either pHHJFH1 or JFH-1 RNA, and then cultured by passaging every 2 or 3 days. As shown in Fig. 3C, both methods of transfection demonstrated similar kinetics of core protein levels until 9 days p.t., after which levels gradually fell. However, significantly greater levels of core protein were detected in the culture of pHHJFH1-transfected cells compared to the RNA-transfected cells on day 12 and 15 p.t. This is likely due to an ongoing production of positive-strand viral RNA from transfected plasmids since RNA degradation generally occurs more quickly than that of circular DNA.

Establishment of stable cell lines constitutively producing HCV virion. To establish cell lines with constitutive HCV production, pHHJFH1/Zeo carrying HCV genomic cDNA and the Zeocin resistance gene were transfected into Huh7.5.1 cells. After approximately 3 weeks of culture with zeocin at a concentration of 0.4 mg/ml, cell colonies producing HCV core protein were screened by ELISA, and three clones were identified that constitutively produced the viral protein (H751JFH1/Zeo cells). Core protein levels within the culture supernatant of selected clones (H751-1, H751-6, and H751-50) were 2.0×10^4, 2.7×10^3, and 1.4×10^3 fmol/liter, respectively. Clone H751-1 was further analyzed. Indirect immunofluorescence with an anti-NS5A antibody showed fluorescent staining of NS5A in the cytoplasm of almost all H751JFH1/

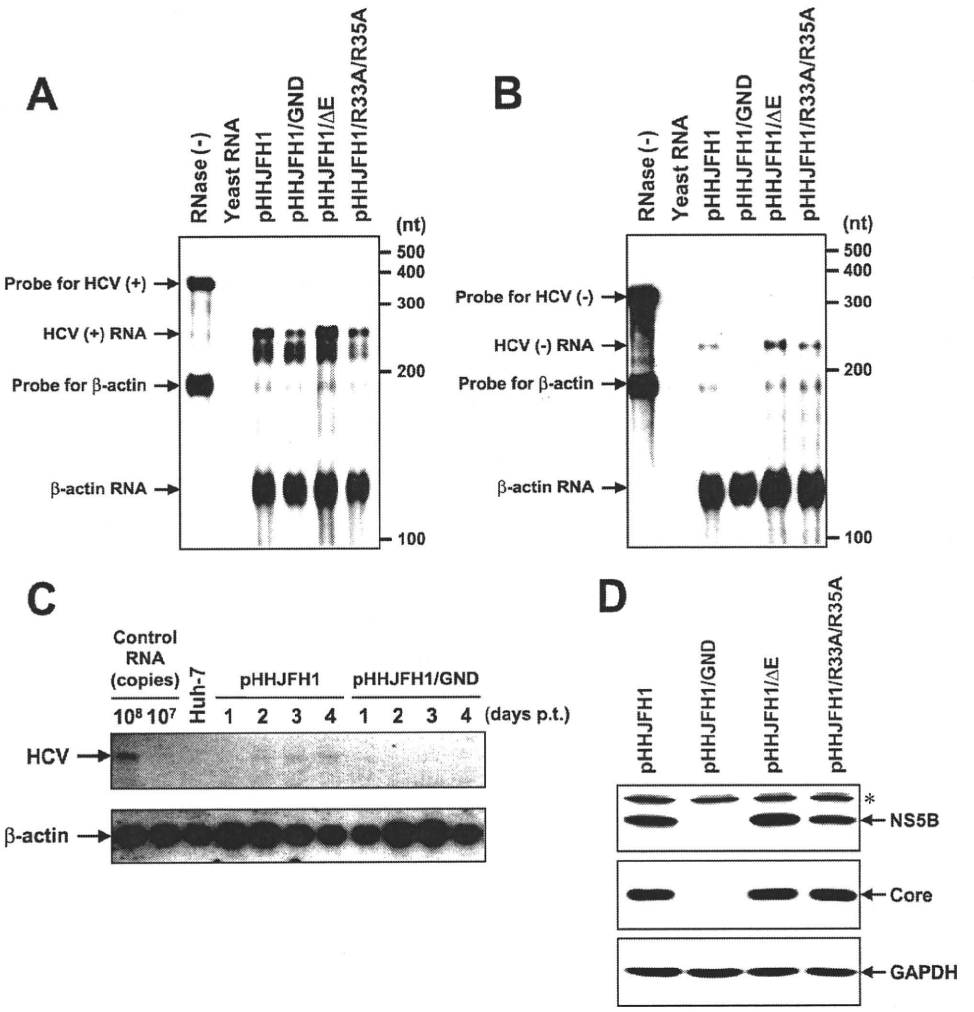

FIG. 2. HCV RNA replication and protein expression in cells transfected with Pol I-driven plasmids. (A and B) Assessment of HCV RNA replication by RPA. Pol I-driven HCV-expression plasmids were transfected into Huh-7 cells. Total RNA was extracted from the cells on day 5 p.t. and positive (A)- and negative (B)-strand HCV RNA levels were determined by RPA as described in Materials and Methods. In the RNase (−) lanes, yeast RNA mixed with RNA probes for HCV and human β-actin were loaded without RNase A/T1 treatment. In the yeast RNA lanes, yeast RNA mixed with RNA probes for HCV and human β-actin were loaded in the presence of RNase A/T1. (C) Northern blotting of total RNAs prepared from the transfected cells. Huh-7 cells transfected with pHHJFH1 or pHHJFH1/GND were harvested for RNA extraction through days 1 to 4 p.t. Control RNA, given numbers of synthetic HCV RNA; Huh-7, RNA extracted from naive cells. Arrows indicate full-length HCV RNA and β-actin RNA. (D) HCV protein expression in the transfected cells. Pol I-driven HCV-expression plasmids were transfected into Huh-7 cells, harvested, and lysed on day 6 p.t. The expression of NS5B, core, and GAPDH was analyzed by Western blotting as described in Materials and Methods. The asterisk indicates nonspecific bands.

Zeo cells (Fig. 4A), whereas no signal was detected in parental Huh7.5.1 cells (Fig. 4B). To determine where HCV RNA replicates in H751JFH1/Zeo cells, labeling of *de novo*-synthesized HCV RNA was performed. After interfering with mRNA production by exposure to actinomycin D, BrUTP-incorporated *de novo*-synthesized HCV RNA was detected in the cytoplasm of H751JFH1/Zeo cells (Fig. 4D) colocalized with NS5A in the perinuclear area (Fig. 4E and F).

Low mutation frequency of the viral genome in a long-term culture of H751JFH1/Zeo cells. The production level of infectious HCV from H751JFH1/Zeo cells at a concentration of $\sim 10^3$ $TCID_{50}$/ml was maintained over 1 year of culture (data not shown). It has been shown that both virus and host cells may adapt during persistent HCV infection in cell cultures, such that cells become resistant to infection due to reduced expression of the viral coreceptor CD81 (54). As shown in Fig. 5, we analyzed the cell surface expression of CD81 on the established cell lines by flow cytometry and observed markedly reduced expression on H751JFH1/Zeo cells compared to parental Huh7.5.1 cells. It is therefore possible that only a small proportion of HCV particles generated from H751JFH1/Zeo cells enter and propagate within the cells. The H751JFH1/Zeo system is thought to result in virtually a single cycle of HCV production from the chromosomally integrated gene and thus

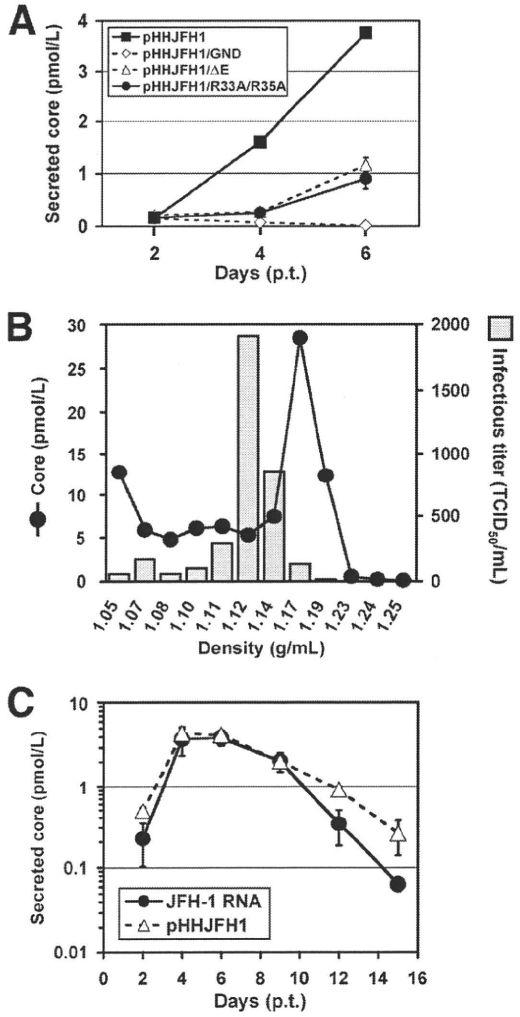

FIG. 3. HCV released from cells transfected with Pol I-driven plasmids. (A) HCV particle secretion from the transfected cells. The culture supernatant of Huh-7 cells transfected with Pol I-driven plasmids containing wild-type or mutated HCV genome were harvested on days 2, 4, and 6 and assayed for HCV core protein levels. The data for each experiment are averages of triplicate values with error bars showing standard deviations. (B) Sucrose density gradient analysis of the culture supernatant of pHHJFH1-transfected cells. Culture supernatant collected on day 5 p.t. was cleared by low-speed centrifugation, passed through a 0.45-μm-pore-size filter, and concentrated ~30-fold by ultrafiltration. After fractionating by sucrose density gradient centrifugation, the core protein level and viral infectious titer of each fraction were measured. (C) Kinetics of core protein secretion from cells transfected with pHHJFH1 or with JFH-1 genomic RNA. A total of 10^6 Huh-7 cells were transfected with 3 μg of pHHJFH1 or the same amount of *in vitro*-transcribed JFH-1 RNA by electroporation. The cells were passaged every 2 to 3 days before reaching confluence. Culture supernatant collected on the indicated days was used for core protein measurement. The level of secreted core protein (pmol/liter) is expressed on a logarithmic scale. The data for each experiment are averages of triplicate values with error bars showing standard deviations.

may yield a virus population with low mutation frequencies. To further examine this, we compared HCV genome mutation rates following production from H751JFH1/Zeo cells compared to cells constitutively infected with HCV after serial passages. RNAs were extracted from the supernatant of H751JFH1/Zeo cells cultured for 120 days, and cDNA sequences were amplified by nested PCR with four sets of primers encompassing almost the entire HCV genome (Table 1). PCR products with expected sizes of 2 to 2.5 kb were obtained [Fig. 6A, RT(+)] and subjected to direct sequencing. No amplified product was detected in samples without reverse transcription [Fig. 6A, RT(−)], suggesting no DNA contamination in culture supernatants or extracted RNA solutions. As shown in Fig. 5B (upper panel), three nucleotide mutations, including two substitutions in the E1 (nt 1218) and E2 (nt 1581) regions, and one deletion in the 3′ UTR (nt 9525) were found within the HCV genome with the mutation rate calculated at 9.6×10^{-4} base substitutions/site/year. These mutations were not detected in the chromosomally integrated HCV cDNA (data not shown). The present results also indicate that no splicing of the viral RNA occurred in the Pol I-based HCV JFH-1 expression system. The HCV genome sequence produced by JFH-1 virus-infected Huh7.5.1 cells was analyzed in the same way using culture supernatant 36 days after RNA transfection. As shown in Fig. 6B (lower panel), 10 mutations, including five substitutions throughout the open reading frame and five deletions in the 3′UTR, were detected, and the mutation rate was calculated at 1.1×10^{-2} base substitutions/site/year.

Effects of glycosylation inhibitors on HCV production. It is known that N-linked glycosylation and oligosaccharide trimming of a variety of viral envelope proteins including HCV E1 and E2 play key roles in the viral maturation and virion production. To evaluate the usefulness of the established cell line for antiviral testing, we determined the effects of glycosylation inhibitors, which have little to no cytotoxicity at the concentrations used, on HCV production in a three day assay using H751JFH1/Zeo cells. The compounds tested are known to inhibit the endoplasmic reticulum (ER), Golgi-resident glucosidases, or mannosidases that trim glucose or mannose residues from N-linked glycans. Some are reported to be involved in proteasome-dependent or -independent degradation of misfolded or unassembled glycoproteins to maintain protein integrity (4, 8, 27, 35).

As shown in Fig. 7A and B, treatment of H751JFH1/Zeo cells with increasing concentrations of *N*N-DNJ, which is an inhibitor of ER α-glucosidases, resulted in a dose-dependent reduction in secreted core protein. *N*N-DNJ was observed to have an IC_{50} (i.e., the concentration inhibiting 50% of core protein secretion) of ~20 μM. In contrast, KIF, which is an ER α-mannosidase inhibitor, resulted in a 1.5- to 2-fold increase in secreted core protein compared to control levels. The other five compounds did not significantly change core protein levels. We further determined the effects of *N*N-DNJ and KIF on the production of infectious HCV (Fig. 7C). As expected, *N*N-DNJ reduced the production of infectious virus in a dose-dependent manner, while production increased in the presence of KIF at 10 to 100 μM. Since *N*N-DNJ and KIF did not significantly influence viral RNA replication, as determined using the subgenomic replicon (data not shown), the present results suggest that some step(s), such as virion assembly, intracellular trafficking, and secretion, may be up- or downregulated depending on glycan modifications of HCV envelope proteins within the ER. Inhibitory effect of *N*N-DNJ was reproducibly observed using the cell line after 1 year of culturing

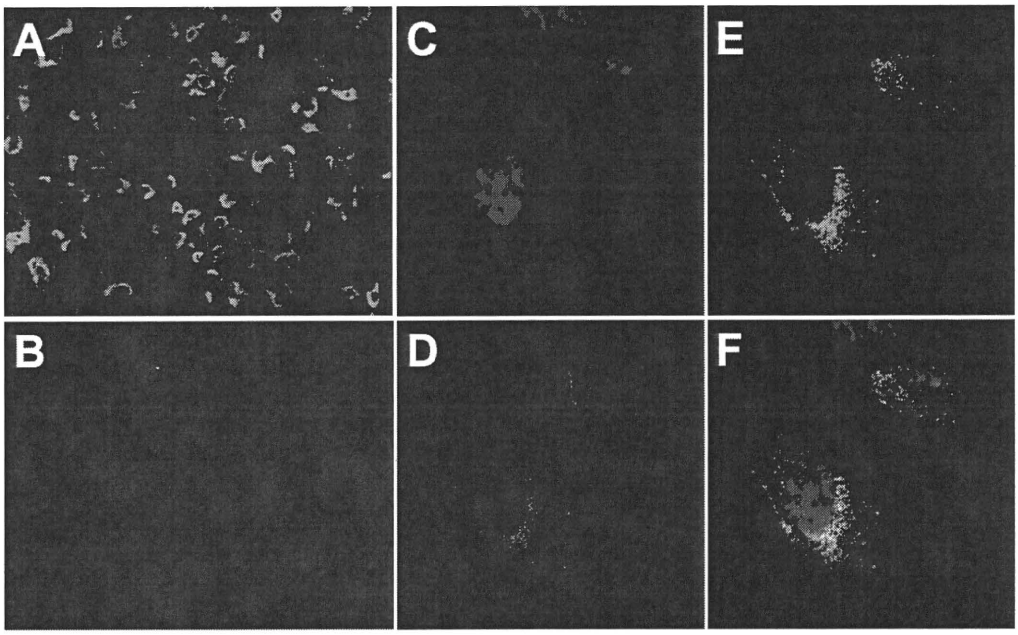

FIG. 4. Indirect immunofluorescence analysis of H751JFH1/Zeo cells. (A and B) H751JFH1/Zeo cells (A) and parental Huh7.5.1 cells (B) were immunostained with an anti-NS5A antibody. (C to F) The subcellular colocalization of *de novo*-synthesized HCV RNA and NS5A in H751JFH1/Zeo cells was analyzed. The cells were stained with DAPI (C), an anti-bromodeoxyuridine antibody (D), and an anti-NS5A antibody (E). The merge panel is shown in panel F.

(Fig. 7D). Under the same condition, the core protein secretion was inhibited by 28 and 58% with 10 and 100 nM BILN 2061, an NS3 protease inhibitor, respectively (Fig. 7D).

Replicon *trans*-packaging system. Recently, ourselves and others have developed a packaging system for HCV subgenomic replicon RNA sequences by providing *trans* viral core-NS2 proteins (1, 17, 41). Since viral structural proteins are not encoded by the subgenomic replicon, progeny virus cannot be produced after transfection. Thus, the single-round infectious HCV-like particle (HCV-LP) generated by this system potentially improves the safety of viral transduction. Here, in order to make the *trans*-packaging system easier to manipulate, we used a Pol I-driven plasmid to develop a transient two-plasmid expression system for the production of HCV-LP. pHH/SGR-Luc, which carries a bicistronic subgenomic reporter replicon with a Pol I promoter/terminator, or its replication-defective mutant, were cotransfected with or without a core-NS2 expression plasmid (Fig. 8A). The culture supernatant was then collected between days 2 and 5 p.t. and used to inoculate naive Huh7.5.1 cells. Reporter luciferase activity, as a quantitative measure of infectious virus production, was assessed in the cells 3 days postinoculation. As shown in Fig. 8B, reporter replication activity was easily detectable in cells inoculated with culture supernatant from cells cotransfected with pHH/

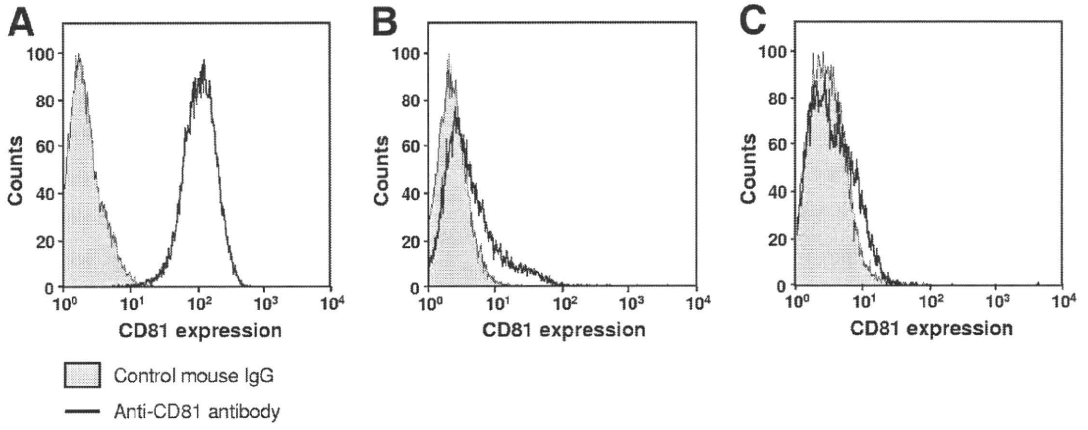

FIG. 5. Loss of CD81 expression in H751JFH1/Zeo cells. The cell surface expression of CD81 on Huh7.5.1 cells (A), H751JFH1/Zeo clone H751-1 (B), and clone H751-50 (C) was analyzed by flow cytometry after being stained with anti-CD81 antibody.

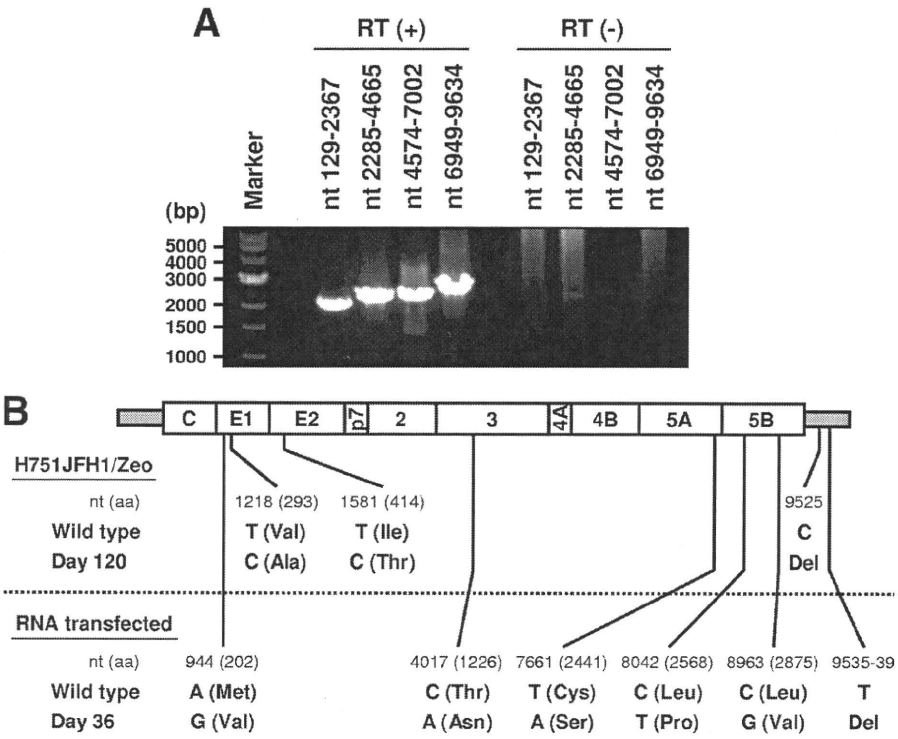

FIG. 6. Genome mutations of HCV secreted from H751JFH1/Zeo cells. (A) RT-PCR of HCV genome extracted from the culture supernatant of H751JFH1/Zeo cells. Viral RNA sequences were reverse transcribed [RT (+)] or not [RT (−)], followed by amplification with primer pairs encompassing the specified HCV genome regions. (B) Comparison of the genome mutations of HCV secreted from H751JFH1/Zeo cells cultured for 120 days (upper panel) and JFH-1 RNA-transfected cells cultured for 36 days (lower panel). The positions of original (wild-type) and mutated (day 120, day 36) nucleotides are indicated under the schematic diagram of the HCV genome. Amino acid residues and their positions are marked in parentheses. Del, deletion.

SGR-Luc and pCAG/C-NS2, with an ~10-fold increase in activity observed at 2 to 5 days p.t. In contrast, luciferase signal in the Huh7.5.1 cells inoculated from supernatant of cells transfected with pHH/SGR-Luc with polymerase-deficient mutation (GND) showed background levels. There was a faint luciferase signal in the cells inoculated from supernatant of cells transfected with pHH/SGR-Luc in the absence of pCAG/C-NS2, suggesting carryover of a low level of cells with the supernatants. Transfer of supernatant from infected cells to naive Huh7.5.1 cells did not result in infection, as judged by undetectable luciferase activity (data not shown). To examine whether NS2 is important for HCV production as previously demonstrated (17–19, 52), we compared the expression of core-NS2 versus core-p7 in the packaged cells (Fig. 8C). The reporter activity in cells inoculated with virus *trans*-packaged by core-p7 was ~100-fold lower than the virus *trans*-packaged by core-NS2, indicating that NS2 needs to be expressed with the structural proteins for efficient assembly and/or infectivity. CD81-dependent infection of HCV-LP was further confirmed by demonstrating reduced reporter activity in the presence of anti-CD81 antibody (Fig. 8D). Thus, we developed a simple *trans*-encapsidation system based on transient two-plasmid transfection, which permits experimental separation of HCV genome replication and virion assembly.

DISCUSSION

Here, we exploited Pol I-derived vectors for expression of the HCV genome, a strategy that generates viral RNAs from the Pol I promoter and terminator. We demonstrated that the HCV JFH-1 RNA produced using this system is unspliced with precise sequences at both ends and that it is replicated in the cytoplasm of transfected cells to produce infectious particles. This approach was used to establish a replicon *trans*-packaging system based on transient two-plasmid transfection and enables the production of a stable cell line capable of constitutive HCV production. The cell line produced using this method can be used to screen a large number of potential antiviral agents by assessing their ability to interfere with HCV replication and/or virion formation. The Pol I-mediated transcription system was originally developed to perform reverse genetics on influenza A viruses (12, 29) which replicate in the nucleus. This system has also been shown useful in the development of reverse genetics for negative-strand RNA viruses having a cytoplasmic replication cycle (3, 10, 11, 31). The results of the present study suggest that the Pol I system can also be used to perform reverse genetics on a cytoplasmically replicating positive-strand RNA virus.

Although viral RNA transfection by electroporation is the most commonly used method to perform reverse genetics on

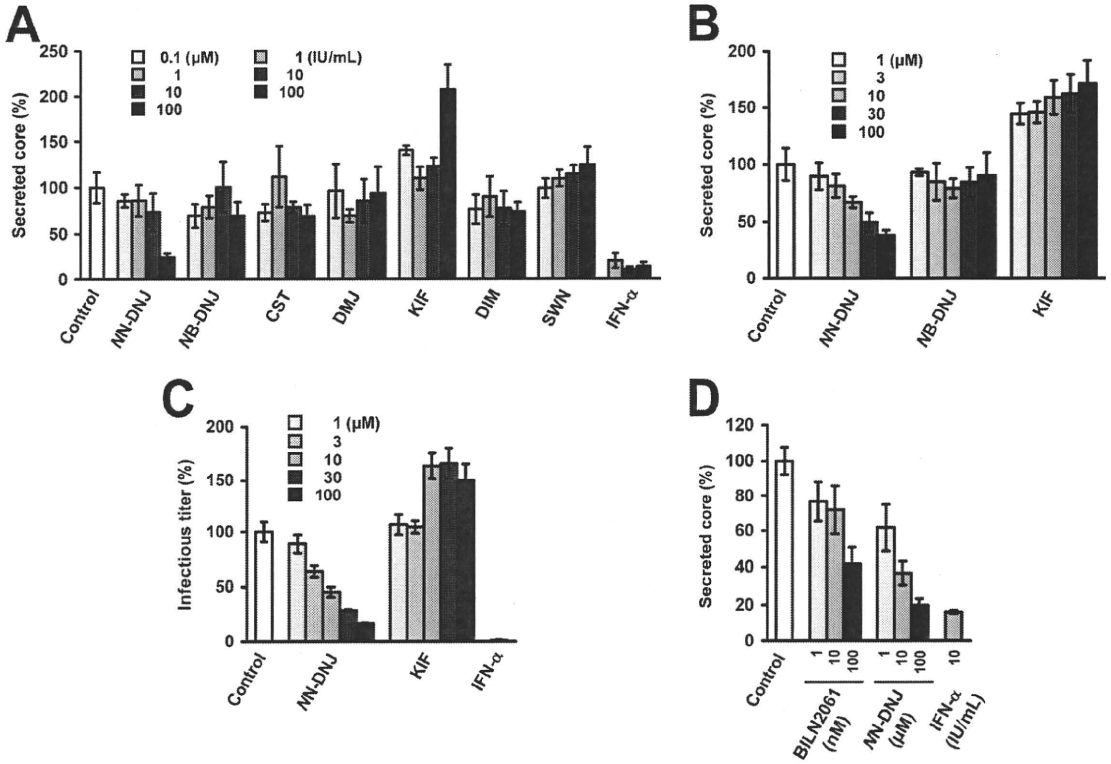

FIG. 7. Effects of glycosylation inhibitors on HCV production from H751JFH1/Zeo cells. (A and B) Effects of glycosylation inhibitors on the secretion of HCV core protein. H751JFH1/Zeo cells were seeded at a density of 1×10^4 cells/well in a 96-well culture plate (A) or 3×10^4 cells/well in a 12-well cell culture plate (B). One day later, each compound was added to the cell culture supernatant at the indicated concentrations. The culture supernatant was collected after a further 3-day culture and processed by core protein-specific ELISA. The control represents an untreated cell culture. The level of secreted core protein was normalized by setting the control value at 100%. The data for each experiment are averages of triplicate values with error bars showing standard deviations. (C) Effects of *N*N-DNJ and KIF on infectious HCV production. The culture supernatant obtained in panel B was used to infect naive Huh7.5.1 cells. At 72 h after infection, the inoculated cells were fixed and immunostained as described in Materials and Methods for titration of virus infectivity. The infectious titer was normalized by setting the control value at 100%. Cells were treated with INF-α at 100 IU/ml as a positive control. The data for each experiment are averages of triplicate values with error bars showing standard deviations. The control represents an untreated cell culture. (D) After 1 year of culturing H751JFH1/Zeo cells, antiviral effects of *N*N-DNJ and BILN 2061 were evaluated. H751JFH1/Zeo cells were seeded at a density of 3×10^4 cells/well in a 12-well cell culture plate. One day later, each compound was added to the cell culture supernatant at the indicated concentrations. The culture supernatant was collected after a further 3-day culture and processed by core protein-specific ELISA. The control represents an untreated cell culture. The level of secreted core protein was normalized by setting the control value at 100%. The data for each experiment are averages of triplicate values with error bars showing standard deviations.

HCV (23, 49, 53), it is comparatively difficult to manipulate. RNA electroporation requires high-quality *in vitro*-synthesized RNA and a large quantity of exponential-growth-phase cells, which may be hard to provide when a number of different RNA constructs are being examined in the same experiment. In addition to the Pol I system, other DNA expression systems have been examined with regard to HCV particle production (5, 15, 21). These systems require ribozyme sequences to be inserted at either end of the HCV genomic cDNA sequence in order to generate appropriately processed viral RNA. However, Heller et al. have reported that the HCV RNA generated by *in vitro* transcription of a HCV-ribozyme plasmid contains uncleaved or prematurely terminated forms of HCV RNA. These authors have also demonstrated that HCV RNA from the culture supernatant of HCV-ribozyme plasmid-transfected cells possesses nucleotide changes at the 5′ and 3′ ends (15), suggesting that the ribozyme is less reliable at generating correct transcripts compared to our Pol I system. In fact, there is evidence to suggest that a mouse Pol I terminator is significantly more effective than an HDV ribozyme in generating precise 3′ ends of RNA, as demonstrated in a plasmid-based influenza virus rescue system (9). Recently, it has been demonstrated that Pol I-catalyzed rRNA transcription is activated in Huh-7 cells following infection with JFH-1 or transfection with a subgenomic HCV replicon (34). HCV NS5A has been shown to upregulate the transcription of Pol I, but not Pol II, through phosphorylation of an upstream binding factor, a Pol I DNA binding transcription factor. These observations indicate that a Pol I-mediated expression system is suitable for efficient production of infectious HCV by DNA transfection.

We established a stable cell line, H751JFH1/Zeo, that constitutively and efficiently produced infectious HCV particles by introducing a Pol I-driven plasmid containing a selection marker into Huh7.5.1 cells. Interestingly, the established cell

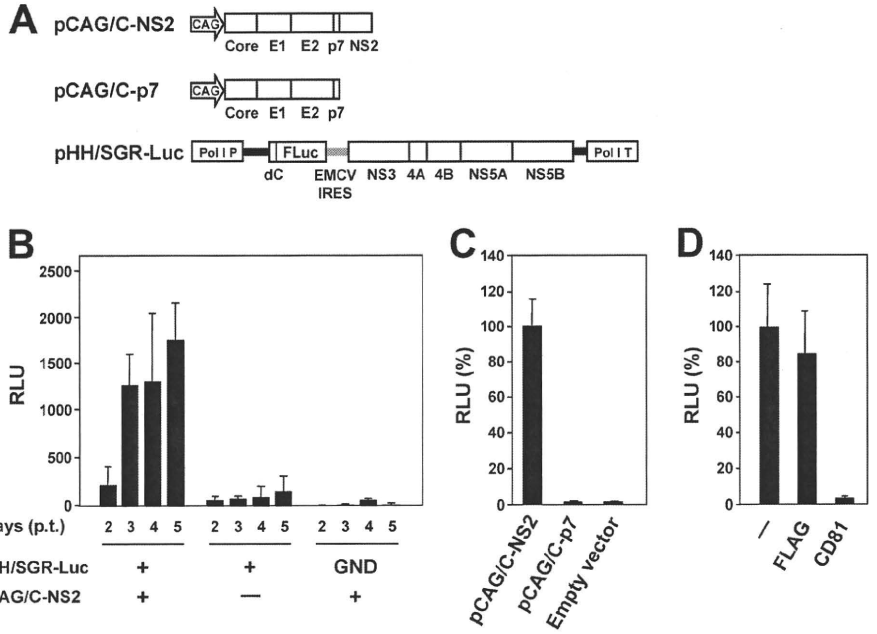

FIG. 8. Establishment of a *trans*-packaging system involving two-plasmid transfection. (A) Schematic representation of the plasmids used for the production of HCV-LP. HCV polyproteins are indicated by the open boxes. Bold lines indicate the HCV UTR. EMCV IRES is denoted by gray bars. The firefly luciferase gene (F Luc) is depicted as a gray box. CAG, CAG promoter; Pol I P, Pol I promoter; dC, 5′ region of Core gene; Pol I T, Pol I terminator. (B) Luciferase activity in Huh7.5.1 cells inoculated with culture supernatant from cells transfected with the indicated plasmids. Luciferase activity is expressed in terms of relative luciferase units (RLU). The data for each experiment are averages of triplicate values with error bars showing standard deviations. (C) Culture supernatant from cells cotransfected with pHH/SGR-Luc and the indicated plasmids were collected 4 days p.t. The luciferase activity in Huh7.5.1 cells inoculated with culture supernatant was determined 3 days postinoculation and expressed as relative luciferase units (RLU). The RLU was normalized according to the luciferase activity observed in the pCAG/C-NS2-transfected sample (C-NS2), which was set at 100%. The data for each experiment are averages of triplicate values with error bars showing standard deviations. (D) Huh7.5.1 cells were inoculated with HCVLP in the absence (−) or presence of 5 μg of anti-CD81 or anti-FLAG antibody/ml. The luciferase activity was determined 72 h postinoculation and is expressed as relative luciferase units (RLU). The RLU was normalized to the level of luciferase activity observed in the antibody-untreated sample (−), which was set at 100%. The data for each experiment are averages of triplicate values with error bars showing standard deviations.

clones exhibited little to no surface expression of CD81, one of the key features of HCV glycoprotein-mediated infection (Fig. 5). Defective expression of receptor molecules might be advantageous in generating stable cell lines for robust production of HCV. HCV-induced cytotoxicity has been reported (7, 45, 54). Persistent HCV infection was established after electroporation of JFH-1 genomic RNA, and a variable cytopathic effect was observed at the peak of acute HCV infection, as well as during the persistent phase of infection (54). A recent study has demonstrated that the cytopathic effect triggered by HCV RNA transfection and viral infection is characterized by massive apoptotic cell death with expression of several ER stress markers, such as GRP78 and phosphorylated eIF2-α (39). Therefore, in the present study, it is likely that selective forces to evade cell death during high levels of HCV replication produced cell populations resistant to virus infection. As a consequence, H751JFH1/Zeo cells maintained robust production of infectious HCV particles over a long period of time without gross cytopathic effects or changes in cell morphology.

Substantial evidence demonstrates that the mutation rate of the HCV genome produced in H751JFH1/Zeo was low (Fig. 6) presumably because of consistent expression of wild-type HCV RNA from the chromosomally integrated gene. Nevertheless, a considerable proportion of the genome was mutated, with two nonsynonymous mutations in the E1 (V293A) and E2 (I414T) regions identified in the culture supernatant of H751JFH1/Zeo cells after 4 months of passages (Fig. 6). A I414T mutation has also been reported after long-term propagation of HCV in culture after JFH-1-RNA transfection (54). This mutation is located between the hypervariable regions 1 and 2 within the N terminus of E2 (51). Adaptive mutations in this region have been shown to enhance virus expansion, presumably by enabling more efficient virus entry (6, 36, 54). A possible CD81-independent mechanism for cell-to-cell transmission of HCV has been proposed (48, 50). However, the mechanisms governing cell-to-cell spread of HCV are not well understood. Further investigation into the importance of envelope protein mutations in HCV transmission independent of CD81 provide a better understanding of the complex interactions required for HCV infection.

In the present study we assessed the effects of N-linked glycosylation inhibitors on HCV production using H751JFH1/Zeo (Fig. 7) and found that an α-glucosidase inhibitor *N*N-DNJ inhibits the production of infectious HCV, which has also been observed in previous studies (43, 47). In contrast, HCV production is increased in the presence of an ER α-mannosidase inhibitor KIF, but not in the presence of the Golgi α-mannosidase inhibitors DMJ, DIM, and SWN. KIF inhibits α-man-

nosidase I, which primarily functions to remove the middle mannose branch from $Man_9GlcNAc_2$ to form $Man_8GlcNAc_2$ after the removal of glucose residues by glucosidases I and II (8, 24). Experiments to elucidate the role of mannose trimming of N-glycans in the HCV life cycle are currently under way.

It has recently been demonstrated that subgenomic replicons or defective genomes of HCV that have the potential of translation and self-replication can be encapsidated into infectious viruslike particles by *trans*-complementation of the viral structural proteins (1, 17, 32, 41, 44). In these studies, the viral RNAs were generally generated by *in vitro* transcription from linearized corresponding plasmids, followed by electroporation into the cells. Structural proteins or Core to NS2 proteins were then provided by DNA or RNA transfection, viral-vector-based transduction, or stable packaging cell lines established. Here, we achieved the replicon *trans*-encapsidation via transient cotransfection with two DNA plasmids. This system, which is apparently easier to manipulate and allows production of *trans*-encapsidated materials more rapidly compared to the systems published, can be applied to the study for understanding phenomenon and biological significance of a variety of naturally occurring HCV subgenomic deletion variants that possibly circulate in hepatitis C patients.

In summary, we have established a Pol I-based reverse-genetics system for the efficient production of infectious HCV. This methodology can be applied to develop (i) a stable HCV-producing cell line with a low mutation frequency of the viral genome and (ii) a simple *trans*-encapsidation system with the flexibility of genome packaging and improved biosafety. This may be useful for antiviral screening and may assist in the development of a live-attenuated HCV vaccine.

ACKNOWLEDGMENTS

We are grateful to Francis V. Chisari (The Scripps Research Institute) for providing Huh7.5.1 cells and to Y. Kawaoka (School of Veterinary Medicine, University of Wisconsin-Madison) for providing the pHH21 vector. We thank A. Murayama and T. Date for their help in sequence and Northern blot analyses and our coworkers for their helpful discussions. We also thank S. Yoshizaki, T. Shimoji, M. Kaga, and M. Sasaki for their technical assistance and T. Mizoguchi for secretarial work.

This study was supported by grants-in-aid from the Ministry of Health, Labor, and Welfare; by the Program for Promotion of Fundamental Studies in Health Sciences of the Organization for Drug ADR Relief, R&D Promotion, and Product Review of Japan (01-3); and by Research on Health Sciences focusing on Drug Innovation from the Japan Health Sciences Foundation, Japan.

REFERENCES

1. **Adair, R., A. H. Patel, L. Corless, S. Griffin, D. J. Rowlands, and C. J. McCormick.** 2009. Expression of hepatitis C virus (HCV) structural proteins in trans facilitates encapsidation and transmission of HCV subgenomic RNA. J. Gen. Virol. **90:**833–842.
2. **Akazawa, D., T. Date, K. Morikawa, A. Murayama, M. Miyamoto, M. Kaga, H. Barth, T. F. Baumert, J. Dubuisson, and T. Wakita.** 2007. CD81 expression is important for the permissiveness of Huh7 cell clones for heterogeneous hepatitis C virus infection. J. Virol. **81:**5036–5045.
3. **Billecocq, A., N. Gauliard, N. Le May, R. M. Elliott, R. Flick, and M. Bouloy.** 2008. RNA polymerase I-mediated expression of viral RNA for the rescue of infectious virulent and avirulent Rift Valley fever viruses. Virology **378:**377–384.
4. **Cabral, C. M., P. Choudhury, Y. Liu, and R. N. Sifers.** 2000. Processing by endoplasmic reticulum mannosidases partitions a secretion-impaired glycoprotein into distinct disposal pathways. J. Biol. Chem. **275:**25015–25022.
5. **Cai, Z., C. Zhang, K. S. Chang, J. Jiang, B. C. Ahn, T. Wakita, T. J. Liang, and G. Luo.** 2005. Robust production of infectious hepatitis C virus (HCV) from stably HCV cDNA-transfected human hepatoma cells. J. Virol. **79:** 13963–13973.
6. **Delgrange, D., A. Pillez, S. Castelain, L. Cocquerel, Y. Rouille, J. Dubuisson, T. Wakita, G. Duverlie, and C. Wychowski.** 2007. Robust production of infectious viral particles in Huh-7 cells by introducing mutations in hepatitis C virus structural proteins. J. Gen. Virol. **88:**2495–2503.
7. **Deng, L., T. Adachi, K. Kitayama, Y. Bungyoku, S. Kitazawa, S. Ishido, I. Shoji, and H. Hotta.** 2008. Hepatitis C virus infection induces apoptosis through a Bax-triggered, mitochondrion-mediated, caspase 3-dependent pathway. J. Virol. **82:**10375–10385.
8. **Ellgaard, L., M. Molinari, and A. Helenius.** 1999. Setting the standards: quality control in the secretory pathway. Science **286:**1882–1888.
9. **Feng, L., F. Li, X. Zheng, W. Pan, K. Zhou, Y. Liu, H. He, and L. Chen.** 2009. The mouse Pol I terminator is more efficient than the hepatitis delta virus ribozyme in generating influenza-virus-like RNAs with precise 3′ ends in a plasmid-only-based virus rescue system. Arch. Virol. **154:**1151–1156.
10. **Flick, R., K. Flick, H. Feldmann, and F. Elgh.** 2003. Reverse genetics for Crimean-Congo hemorrhagic fever virus. J. Virol. **77:**5997–6006.
11. **Flick, R., and R. F. Pettersson.** 2001. Reverse genetics system for Uukuniemi virus (*Bunyaviridae*): RNA polymerase I-catalyzed expression of chimeric viral RNAs. J. Virol. **75:**1643–1655.
12. **Fodor, E., L. Devenish, O. G. Engelhardt, P. Palese, G. G. Brownlee, and A. Garcia-Sastre.** 1999. Rescue of influenza A virus from recombinant DNA. J. Virol. **73:**9679–9682.
13. **Groseth, A., H. Feldmann, S. Theriault, G. Mehmetoglu, and R. Flick.** 2005. RNA polymerase I-driven minigenome system for Ebola viruses. J. Virol. **79:**4425–4433.
14. **Hamamoto, I., Y. Nishimura, T. Okamoto, H. Aizaki, M. Liu, Y. Mori, T. Abe, T. Suzuki, M. M. Lai, T. Miyamura, K. Moriishi, and Y. Matsuura.** 2005. Human VAP-B is involved in hepatitis C virus replication through interaction with NS5A and NS5B. J. Virol. **79:**13473–13482.
15. **Heller, T., S. Saito, J. Auerbach, T. Williams, T. R. Moreen, A. Jazwinski, B. Cruz, N. Jeurkar, R. Sapp, G. Luo, and T. J. Liang.** 2005. An in vitro model of hepatitis C virion production. Proc. Natl. Acad. Sci. U. S. A. **102:**2579–2583.
16. **Hoofnagle, J. H.** 2002. Course and outcome of hepatitis C. Hepatology **36:**S21–S29.
17. **Ishii, K., K. Murakami, S. S. Hmwe, B. Zhang, J. Li, M. Shirakura, K. Morikawa, R. Suzuki, T. Miyamura, T. Wakita, and T. Suzuki.** 2008. Trans-encapsidation of hepatitis C virus subgenomic replicon RNA with viral structure proteins. Biochem. Biophys. Res. Commun. **371:**446–450.
18. **Jirasko, V., R. Montserret, N. Appel, A. Janvier, L. Eustachi, C. Brohm, E. Steinmann, T. Pietschmann, F. Penin, and R. Bartenschlager.** 2008. Structural and functional characterization of nonstructural protein 2 for its role in hepatitis C virus assembly. J. Biol. Chem. **283:**28546–28562.
19. **Jones, C. T., C. L. Murray, D. K. Eastman, J. Tassello, and C. M. Rice.** 2007. Hepatitis C virus p7 and NS2 proteins are essential for production of infectious virus. J. Virol. **81:**8374–8383.
20. **Kato, T., T. Date, M. Miyamoto, M. Sugiyama, Y. Tanaka, E. Orito, T. Ohno, K. Sugihara, I. Hasegawa, K. Fujiwara, K. Ito, A. Ozasa, M. Mizokami, and T. Wakita.** 2005. Detection of anti-hepatitis C virus effects of interferon and ribavirin by a sensitive replicon system. J. Clin. Microbiol. **43:**5679–5684.
21. **Kato, T., T. Matsumura, T. Heller, S. Saito, R. K. Sapp, K. Murthy, T. Wakita, and T. J. Liang.** 2007. Production of infectious hepatitis C virus of various genotypes in cell cultures. J. Virol. **81:**4405–4411.
22. **Liang, T. J., B. Rehermann, L. B. Seeff, and J. H. Hoofnagle.** 2000. Pathogenesis, natural history, treatment, and prevention of hepatitis C. Ann. Intern. Med. **132:**296–305.
23. **Lindenbach, B. D., M. J. Evans, A. J. Syder, B. Wolk, T. L. Tellinghuisen, C. C. Liu, T. Maruyama, R. O. Hynes, D. R. Burton, J. A. McKeating, and C. M. Rice.** 2005. Complete replication of hepatitis C virus in cell culture. Science **309:**623–626.
24. **Liu, Y., P. Choudhury, C. M. Cabral, and R. N. Sifers.** 1999. Oligosaccharide modification in the early secretory pathway directs the selection of a misfolded glycoprotein for degradation by the proteasome. J. Biol. Chem. **274:** 5861–5867.
25. **Manns, M. P., H. Wedemeyer, and M. Cornberg.** 2006. Treating viral hepatitis C: efficacy, side effects, and complications. Gut **55:**1350–1359.
26. **Masaki, T., R. Suzuki, K. Murakami, H. Aizaki, K. Ishii, A. Murayama, T. Date, Y. Matsuura, T. Miyamura, T. Wakita, and T. Suzuki.** 2008. Interaction of hepatitis C virus nonstructural protein 5A with core protein is critical for the production of infectious virus particles. J. Virol. **82:**7964–7976.
27. **Meusser, B., C. Hirsch, E. Jarosch, and T. Sommer.** 2005. ERAD: the long road to destruction. Nat. Cell Biol. **7:**766–772.
28. **Neumann, G., and Y. Kawaoka.** 2001. Reverse genetics of influenza virus. Virology **287:**243–250.
29. **Neumann, G., T. Watanabe, H. Ito, S. Watanabe, H. Goto, P. Gao, M. Hughes, D. R. Perez, R. Donis, E. Hoffmann, G. Hobom, and Y. Kawaoka.** 1999. Generation of influenza A viruses entirely from cloned cDNAs. Proc. Natl. Acad. Sci. U. S. A. **96:**9345–9350.
30. **Niwa, H., K. Yamamura, and J. Miyazaki.** 1991. Efficient selection for high-expression transfectants with a novel eukaryotic vector. Gene **108:**193–199.
31. **Ogawa, Y., K. Sugiura, K. Kato, Y. Tohya, and H. Akashi.** 2007. Rescue of

Akabane virus (family *Bunyaviridae*) entirely from cloned cDNAs by using RNA polymerase I. J. Gen. Virol. **88:**3385–3390.
32. **Pacini, L., R. Graziani, L. Bartholomew, R. De Francesco, and G. Paonessa.** 2009. Naturally occurring hepatitis C virus subgenomic deletion mutants replicate efficiently in Huh-7 cells and are trans-packaged in vitro to generate infectious defective particles. J. Virol. **83:**9079–9093.
33. **Poynard, T., M. F. Yuen, V. Ratziu, and C. L. Lai.** 2003. Viral hepatitis C. Lancet **362:**2095–2100.
34. **Raychaudhuri, S., V. Fontanes, B. Barat, and A. Dasgupta.** 2009. Activation of rRNA transcription by hepatitis C virus involves upstream binding factor phosphorylation via induction of cyclin D1. Cancer Res. **69:**2057–2064.
35. **Ruddock, L. W., and M. Molinari.** 2006. N-glycan processing in ER quality control. J. Cell Sci. **119:**4373–4380.
36. **Russell, R. S., J. C. Meunier, S. Takikawa, K. Faulk, R. E. Engle, J. Bukh, R. H. Purcell, and S. U. Emerson.** 2008. Advantages of a single-cycle production assay to study cell culture-adaptive mutations of hepatitis C virus. Proc. Natl. Acad. Sci. U. S. A. **105:**4370–4375.
37. **Seeff, L. B., and J. H. Hoofnagle.** 2003. Appendix: National Institutes of Health Consensus Development Conference Management of Hepatitis C 2002. Clin. Liver Dis. **7:**261–287.
38. **Seeff, L. B., and J. H. Hoofnagle.** 2002. National Institutes of Health Consensus Development Conference: management of hepatitis C: 2002. Hepatology **36:**S1–S2.
39. **Sekine-Osajima, Y., N. Sakamoto, K. Mishima, M. Nakagawa, Y. Itsui, M. Tasaka, Y. Nishimura-Sakurai, C. H. Chen, T. Kanai, K. Tsuchiya, T. Wakita, N. Enomoto, and M. Watanabe.** 2008. Development of plaque assays for hepatitis C virus-JFH1 strain and isolation of mutants with enhanced cytopathogenicity and replication capacity. Virology **371:**71–85.
40. **Shi, S. T., K. J. Lee, H. Aizaki, S. B. Hwang, and M. M. Lai.** 2003. Hepatitis C virus RNA replication occurs on a detergent-resistant membrane that cofractionates with caveolin-2. J. Virol. **77:**4160–4168.
41. **Steinmann, E., C. Brohm, S. Kallis, R. Bartenschlager, and T. Pietschmann.** 2008. Efficient trans-encapsidation of hepatitis C virus RNAs into infectious virus-like particles. J. Virol. **82:**7034–7046.
42. **Steinmann, E., F. Penin, S. Kallis, A. H. Patel, R. Bartenschlager, and T. Pietschmann.** 2007. Hepatitis C virus p7 protein is crucial for assembly and release of infectious virions. PLoS Pathog. **3:**e103.
43. **Steinmann, E., T. Whitfield, S. Kallis, R. A. Dwek, N. Zitzmann, T. Pietschmann, and R. Bartenschlager.** 2007. Antiviral effects of amantadine and iminosugar derivatives against hepatitis C virus. Hepatology **46:**330–338.
44. **Sugiyama, K., K. Suzuki, T. Nakazawa, K. Funami, T. Hishiki, K. Ogawa, S. Saito, K. W. Shimotohno, T. Suzuki, Y. Shimizu, R. Tobita, M. Hijikata, H. Takaku, and K. Shimotohno.** 2009. Genetic analysis of hepatitis C virus with defective genome and its infectivity in vitro. J. Virol. **83:**6922–6928.
45. **Sung, V. M., S. Shimodaira, A. L. Doughty, G. R. Picchio, H. Can, T. S. Yen, K. L. Lindsay, A. M. Levine, and M. M. Lai.** 2003. Establishment of B-cell lymphoma cell lines persistently infected with hepatitis C virus in vivo and in vitro: the apoptotic effects of virus infection. J. Virol. **77:**2134–2146.
46. **Suzuki, T., K. Ishii, H. Aizaki, and T. Wakita.** 2007. Hepatitis C viral life cycle. Adv. Drug Deliv. Rev. **59:**1200–1212.
47. **Tani, H., Y. Komoda, E. Matsuo, K. Suzuki, I. Hamamoto, T. Yamashita, K. Moriishi, K. Fujiyama, T. Kanto, N. Hayashi, A. Owsianka, A. H. Patel, M. A. Whitt, and Y. Matsuura.** 2007. Replication-competent recombinant vesicular stomatitis virus encoding hepatitis C virus envelope proteins. J. Virol. **81:**8601–8612.
48. **Timpe, J. M., Z. Stamataki, A. Jennings, K. Hu, M. J. Farquhar, H. J. Harris, A. Schwarz, I. Desombere, G. L. Roels, P. Balfe, and J. A. McKeating.** 2008. Hepatitis C virus cell-cell transmission in hepatoma cells in the presence of neutralizing antibodies. Hepatology **47:**17–24.
49. **Wakita, T., T. Pietschmann, T. Kato, T. Date, M. Miyamoto, Z. Zhao, K. Murthy, A. Habermann, H. G. Krausslich, M. Mizokami, R. Bartenschlager, and T. J. Liang.** 2005. Production of infectious hepatitis C virus in tissue culture from a cloned viral genome. Nat. Med. **11:**791–796.
50. **Witteveldt, J., M. J. Evans, J. Bitzegeio, G. Koutsoudakis, A. M. Owsianka, A. G. Angus, Z. Y. Keck, S. K. Foung, T. Pietschmann, C. M. Rice, and A. H. Patel.** 2009. CD81 is dispensable for hepatitis C virus cell-to-cell transmission in hepatoma cells. J. Gen. Virol. **90:**48–58.
51. **Yagnik, A. T., A. Lahm, A. Meola, R. M. Roccasecca, B. B. Ercole, A. Nicosia, and A. Tramontano.** 2000. A model for the hepatitis C virus envelope glycoprotein E2. Proteins **40:**355–366.
52. **Yi, M., Y. Ma, J. Yates, and S. M. Lemon.** 2009. Trans-complementation of an NS2 defect in a late step in hepatitis C virus (HCV) particle assembly and maturation. PLoS Pathog. **5:**e1000403.
53. **Zhong, J., P. Gastaminza, G. Cheng, S. Kapadia, T. Kato, D. R. Burton, S. F. Wieland, S. L. Uprichard, T. Wakita, and F. V. Chisari.** 2005. Robust hepatitis C virus infection in vitro. Proc. Natl. Acad. Sci. U. S. A. **102:**9294–9299.
54. **Zhong, J., P. Gastaminza, J. Chung, Z. Stamataki, M. Isogawa, G. Cheng, J. A. McKeating, and F. V. Chisari.** 2006. Persistent hepatitis C virus infection in vitro: coevolution of virus and host. J. Virol. **80:**11082–11093.

Virology 405 (2010) 361–369

Contents lists available at ScienceDirect

Virology

journal homepage: www.elsevier.com/locate/yviro

Cell culture and in vivo analyses of cytopathic hepatitis C virus mutants☆,☆☆

Kako Mishima [a,1], Naoya Sakamoto [a,b,*,1], Yuko Sekine-Osajima [a], Mina Nakagawa [a,b], Yasuhiro Itsui [a,c], Seishin Azuma [a], Sei Kakinuma [a,b], Kei Kiyohashi [a], Akiko Kitazume [a], Kiichiro Tsuchiya [a], Michio Imamura [d], Nobuhiko Hiraga [d], Kazuaki Chayama [d], Takaji Wakita [e], Mamoru Watanabe [a]

[a] Department of Gastroenterology and Hepatology, Tokyo Medical and Dental University, 1-5-45 Yushima, Bunkyo-ku, Tokyo 113-8519, Japan
[b] Department for Hepatitis Control, Tokyo Medical and Dental University, 1-5-45 Yushima, Bunkyo-ku, Tokyo 113-8519, Japan
[c] Department of Internal Medicine, Soka Municipal Hospital, 2-21-1 Soka, Soka City, Saitama 340-8560, Japan
[d] Department of Medicine and Molecular Science, Division of Frontier Medical Science, Programs for Biomedical Research, Graduate School of Biomedical Sciences, Hiroshima University, 1-2-3 Kasumi, Minami-ku, Hiroshima City, Hiroshima 734-8551, Japan
[e] Department of Virology II, National Institute of Infectious Diseases, 1-23-1 Toyama, Shinjuku-ku, Tokyo 162-8640, Japan

ARTICLE INFO

Article history:
Received 11 March 2010
Returned to author for revision 7 April 2010
Accepted 7 June 2010
Available online 6 July 2010

Keywords:
HCV-JFH1 cell culture
Plaque assay
Cytopathic effect
Adaptive mutations
Human hepatocyte chimeric mice

ABSTRACT

HCV-JFH1 yields subclones that develop cytopathic plaques (Sekine-Osajima Y, et al., Virology 2008; 371:71). Here, we investigated viral amino acid substitutions in cytopathic mutant HCV-JFH1 clones and their characteristics in vitro and in vivo. The mutant viruses with individual C2441S, P2938S or R2985P signature substitutions, and with all three substitutions, showed significantly higher intracellular replication efficiencies and greater cytopathic effects than the parental JFH1 in vitro. The mutant HCV-inoculated mice showed significantly higher serum HCV RNA and higher level of expression of ER stress-related proteins in early period of infection. At 8 weeks post inoculation, these signature mutations had reverted to the wild type sequences. HCV-induced cytopathogenicity is associated with the level of intracellular viral replication and is determined by certain amino acid substitutions in HCV-NS5A and NS5B regions. The cytopathic HCV clones exhibit high replication competence in vivo but may be eliminated during the early stages of infection.

Introduction

Hepatitis C virus (HCV) is one of the most important pathogens causing liver-related morbidity and mortality (Alter, 1997). Antiviral therapeutic options against HCV have been limited to type I interferons and ribavirin and have yielded unsatisfactory responses (Fried et al., 2002). Given this situation, a precise understanding of the molecular mechanisms of interferon resistance has been a high priority of research in academia and industry.

Molecular analyses of the HCV life cycle, virus–host interactions, and mechanisms of liver cell damage by the virus are not understood completely, mainly because of the lack of cell culture systems. These problems have been overcome to some extent by the development of the HCV subgenomic replicon (Lohmann et al., 1999) and HCV cell culture systems (Lindenbach et al., 2005; Wakita et al., 2005; Zhong et al., 2005). The HCV-JFH1 strain, which is a genotype 2a clone derived from a Japanese fulminant hepatitis patient and can replicate efficiently in Huh7 cells (Kato, 2001; Kato et al., 2003), has contributed to the establishment of the HCV cell culture system. Furthermore, the Huh7-derived cell lines, Huh-7.5 and Huh-7.5.1 cells, allow production of higher viral titers and have a greater permissivity for HCV (Koutsoudakis et al., 2007; Lindenbach et al., 2005; Zhong et al., 2005). The HCV-JFH1 cell culture system now allows us to study the complete HCV life cycle: virus–cell entry, translation, protein processing, RNA replication, virion assembly and virus release.

HCV belongs to the family *Flaviviridae*. One of the characteristics of the *Flaviviridae* is that they cause cytopathic effects (CPE). The viruses have positive strand RNA genomes of ~10 kilo-bases that encode polyproteins of ~3000 amino acids. These proteins are processed post-translationally by cellular and viral proteases into at least 10 mature proteins (Sakamoto and Watanabe, 2009). The viral non-structural proteins accumulate in the ER and direct genomic replication and viral protein synthesis (Bartenschlager and Lohmann, 2000; Jordan et al., 2002; Mottola et al., 2002). It has been recently

Abbreviations: HCV, hepatitis C virus; CPE, cytopathic effect; ER, endoplasmic reticulum; RdRp, RNA dependent RNA polymerase.

☆ The authors, K.M., N.S., Y.S., M.N., Y.I., S.A., S.K., K.K., A.K., K.T., M.I., N.H., K.C., T.W. and M.W. declare that there is no conflict of interest.

☆☆This study was supported by grants from Ministry of Education, Culture, Sports, Science and Technology-Japan, the Japan Society for the Promotion of Science, Ministry of Health, Labour and Welfare-Japan, Japan Health Sciences Foundation, and National Institute of Biomedical Innovation.

* Corresponding author. Department of Gastroenterology and Hepatology, Tokyo Medical and Dental University, 1-5-45 Yushima, Bunkyo-ku, Tokyo 113-8519, Japan. Fax: +81 3 5803 0268.
E-mail address: nsakamoto.gast@tmd.ac.jp (N. Sakamoto).

[1] K. M. and N. S. contributed equally to this work.

0042-6822/$ – see front matter © 2010 Elsevier Inc. All rights reserved.
doi:10.1016/j.virol.2010.06.020